

# Measurement of Full-Sky Cosmic-Ray Anisotropy with HAWC and IceCube

Juan Carlos Díaz Vélez<sup>a,b</sup>,  
M. Ahlers<sup>c</sup>, D. Fiorino<sup>d</sup>, P. Desiati<sup>b</sup>

APS April Meeting

April 13, 2019

Denver, Colorado

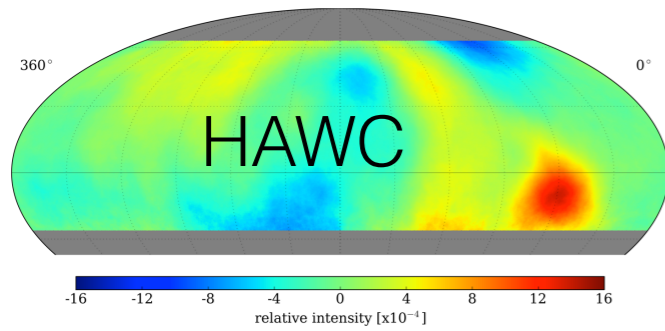
<sup>a</sup>Centro Universitario de los Valles, Universidad de Guadalajara, Guadalajara, Jalisco, México

<sup>b</sup>Wisconsin IceCube Particle Astrophysics Center (WIPAC) and Department of Physics, University of Wisconsin–Madison, Madison, WI 53706, USA

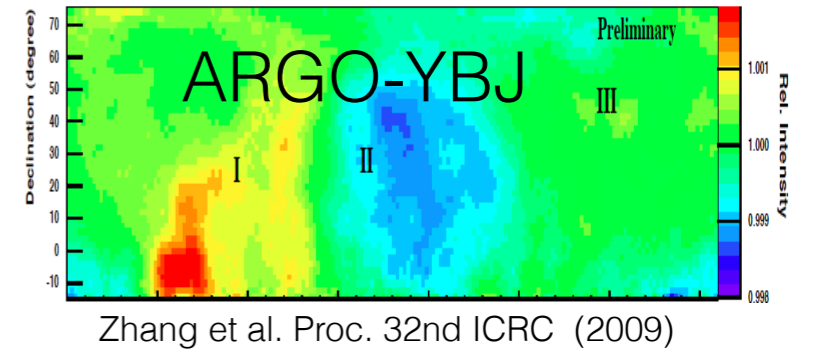
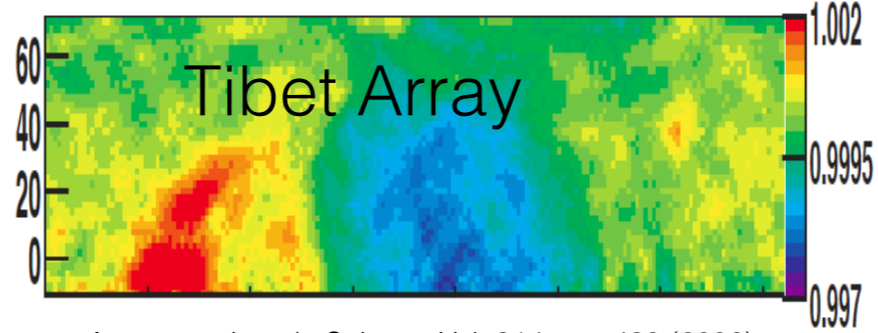
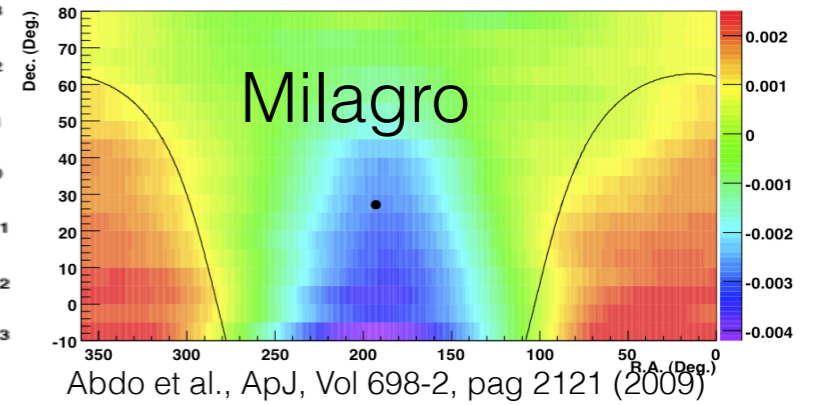
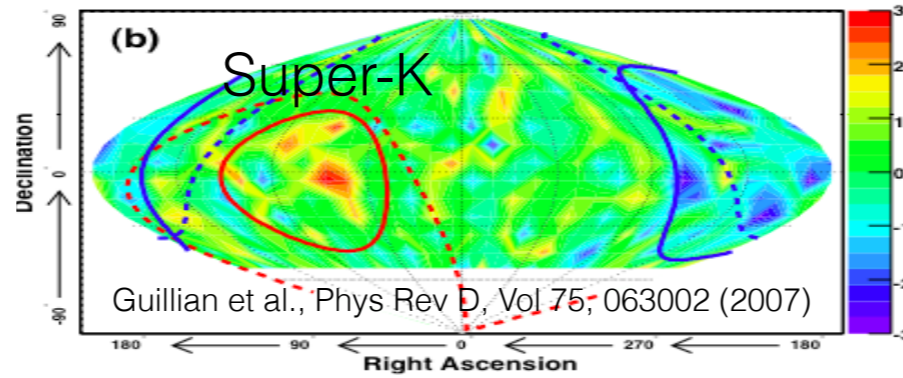
<sup>c</sup>Niels Bohr Institute, University of Copenhagen, Copenhagen, Denmark

<sup>d</sup>Department of Physics, University of Maryland, College Park, MD, USA

Over the last few decades, several studies have measured a large scale anisotropy at  $10^{-3}$  level and a small-scale structure with an amplitude of  $10^{-4}$  and angular size from  $10^\circ$  to  $30^\circ$ .

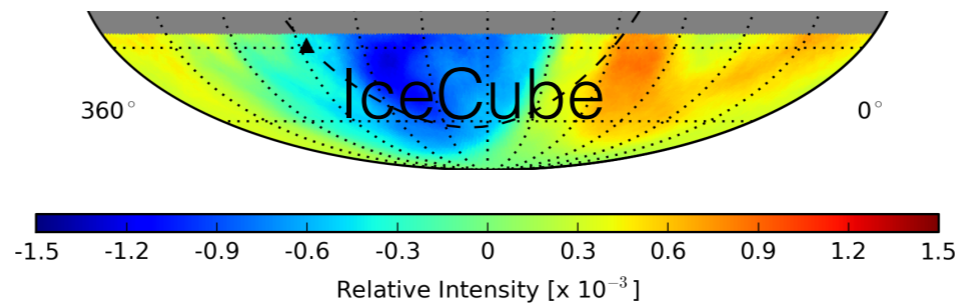


A. U. Abeysekara et al. *Astrophys. J.* (2014)



North

South



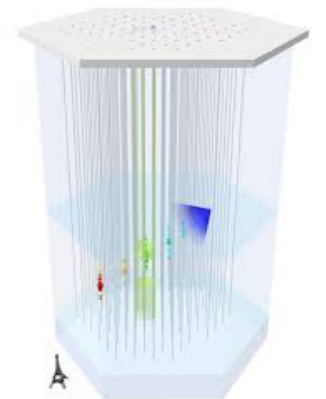
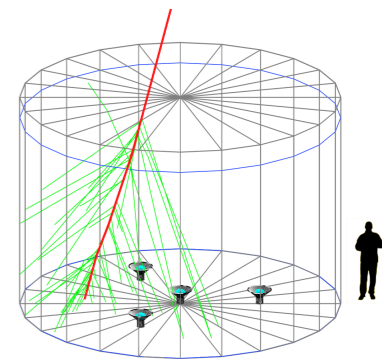
M. G. Aartsen et al. *Astrophys. J.* 826 (2016)

Large-scale features in South appear to be a continuation of those observed in the Northern Hemisphere.

# The IceCube and HAWC Data Sets

Individual experiments have provided partial sky coverage that limits the interpretation of the results. This first full-sky combined observation at the same energy is done with two observatories covering most of the celestial sphere.

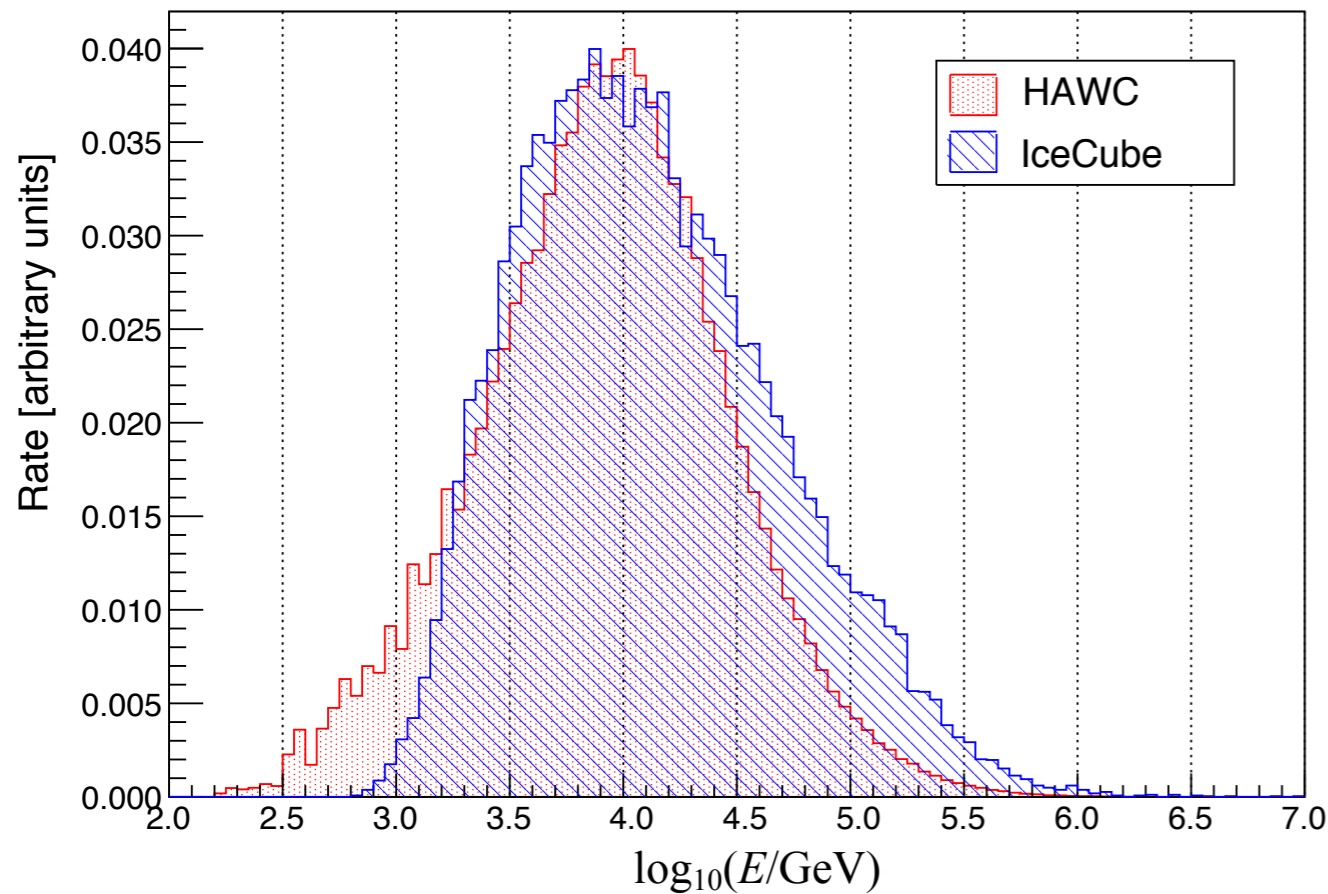
	<b>IceCube</b>		<b>HAWC</b>	
Hemisphere	Southern		Northern	
Latitude	-90°		19°	
Detection method	muons produced by CR		air showers produced by CR and $\gamma$	
Field of view	-90°/-20°, ~4 sr (same sky over 24h)		-30° /68° , ~2 sr (8 sr observed)/24 h	
Livetime	5 years		519 days over a period of 653 days	
Detector trigger rate	2.5 kHz		25 kHz	
	quality cuts	energy cuts	quality cuts	energy cuts
Median primary energy	20 TeV	10 TeV	2 TeV	10 TeV
Approx. angular	2-3°	2-6°	0.3-1.5°	0.3-1.5°
Events	$2.8 \times 10^{11}$	$1.7 \times 10^{11}$	$7.1 \times 10^{10}$	$2.8 \times 10^{10}$



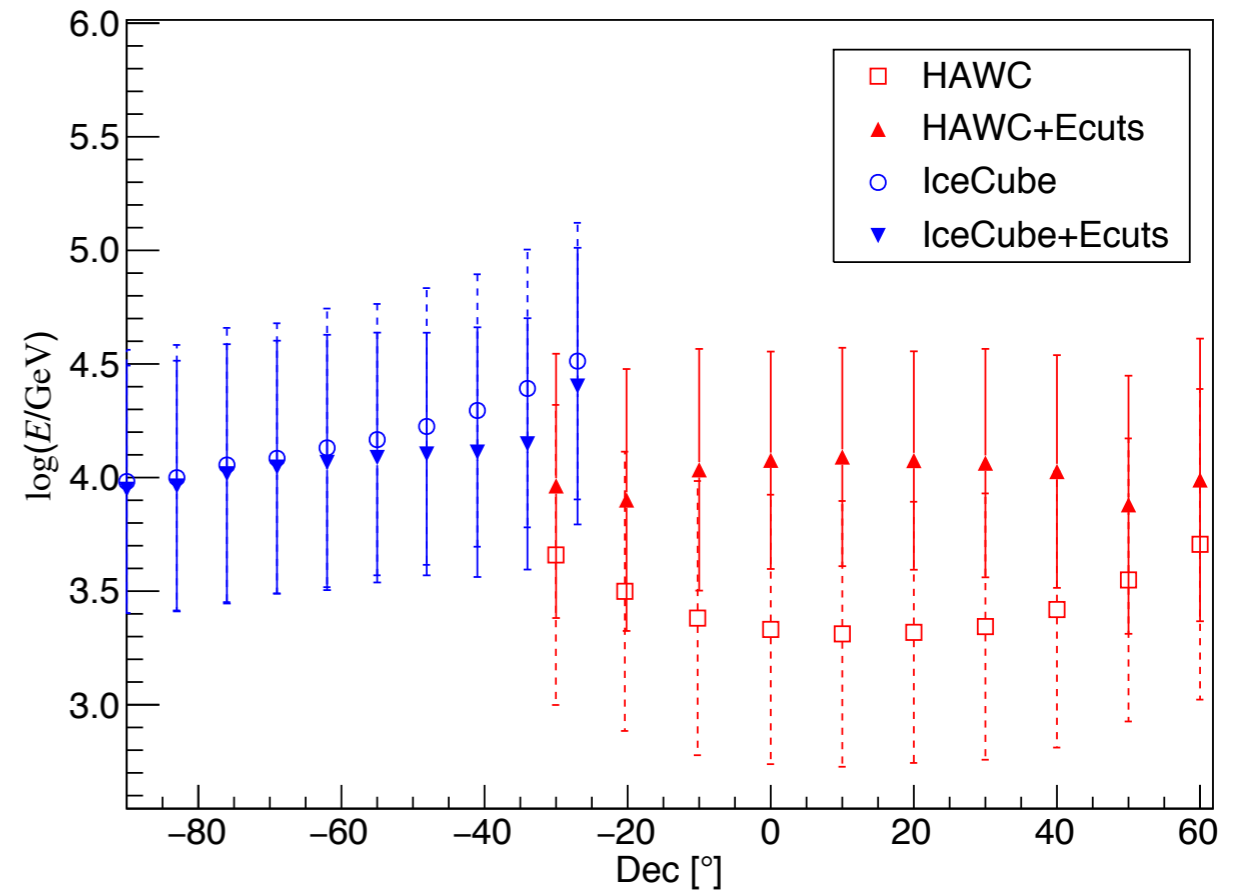
Data selected for analysis come from IC86 2011-2015, as well as 2 years of HAWC in its final configuration of 300 tanks (HAWC300). Only continuous sidereal days\* of data were chosen for these analyses in order to reduce the bias of uneven exposure along right ascension.

\* Gaps of 20 min. allowed within each 24 h period

## Energy Distribution (MC)



## Median Energy



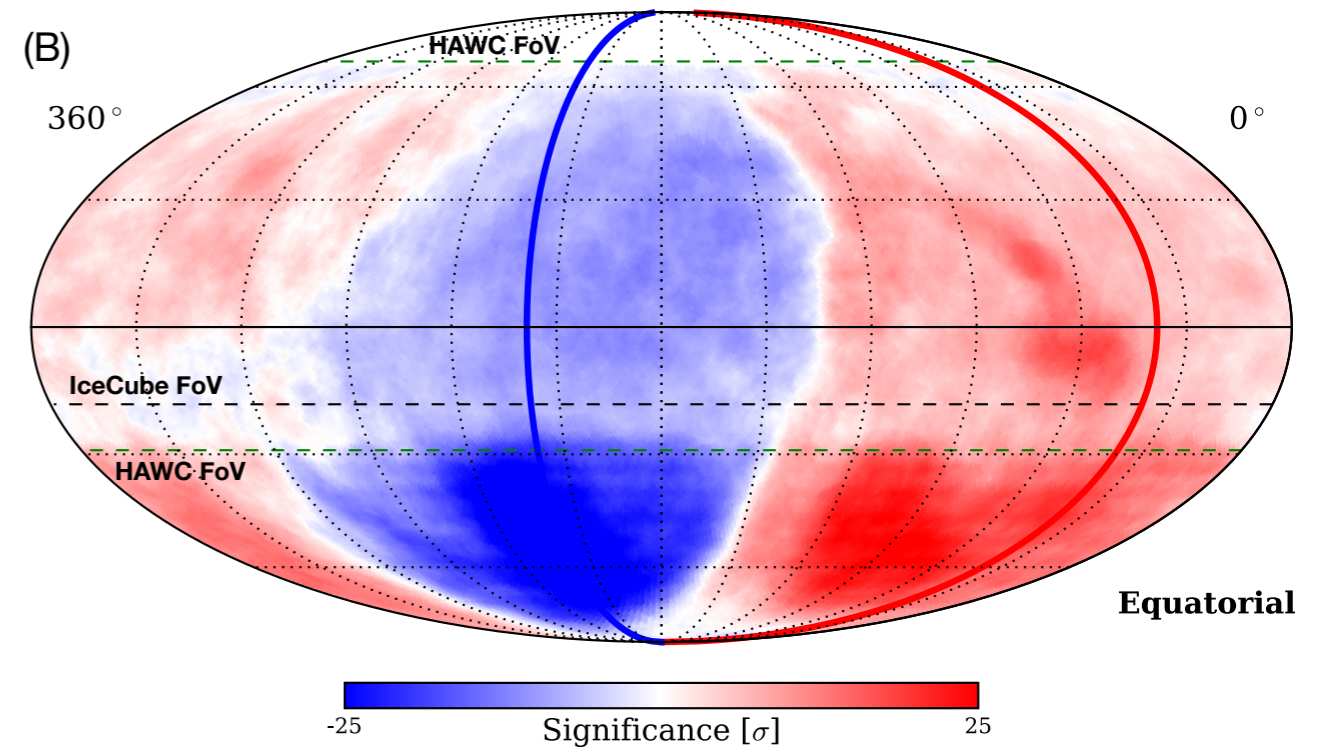
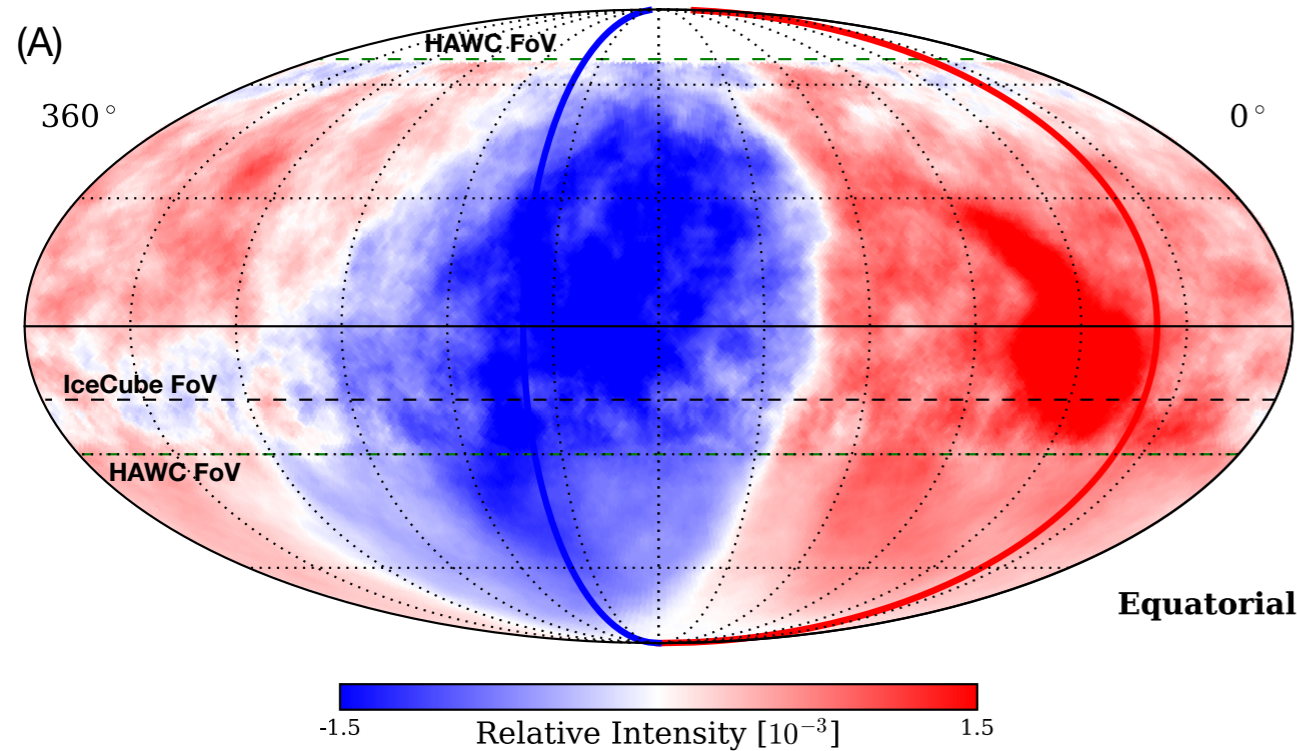
The resulting energy distribution of the two datasets after applying energy cuts is shown on the left above. After cuts, both CR data sets have a median energy of approximately 10 TeV with little dependence on zenith angle. Before cuts, the median energy grows as a function of shower zenith angle and is largest in the narrow region of overlap between the two detectors.

## Composition (MC)

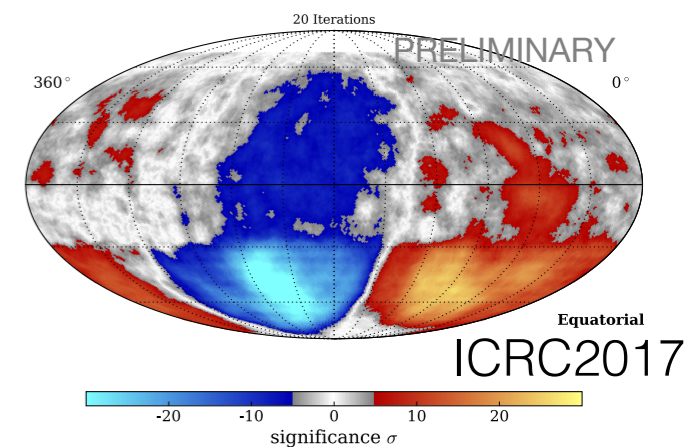
	IceCube	HAWC
Proton	0.756	0.616
He	0.195	0.311
CNO	0.028	0.047
NeMgSi	0.013	0.019
Fe	0.008	0.008

# Relative Intensity

# Significance Map



- Relative intensity and significance maps after 20 iterations smoothed over  $5^\circ$  radius.
- **First full-sky combined observation at same energy with two observatories covering most of the celestial sphere.**
- Caveat: Background estimation suppresses sensitivity to z component of the anisotropy.



# 2D Fit

Summary plot (adopted from M. Ahlers et al. ArXiv.1612.01873) of the reconstructed TeV-PeV dipole amplitude and phase.

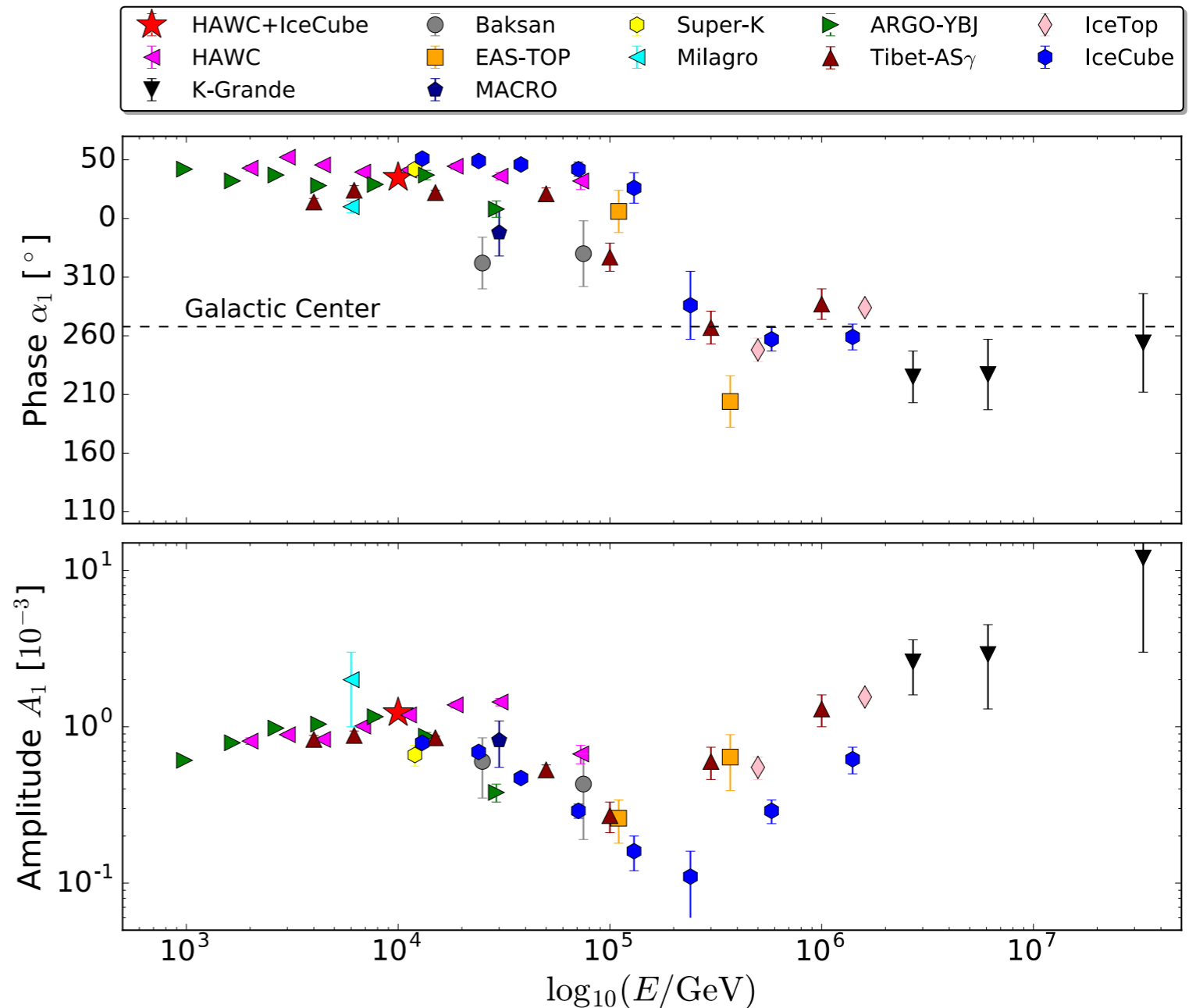
$$A_1 = 1.17e-3 \pm .01e-3$$

$$\alpha_1 = 38.4^\circ \pm 0.3^\circ$$

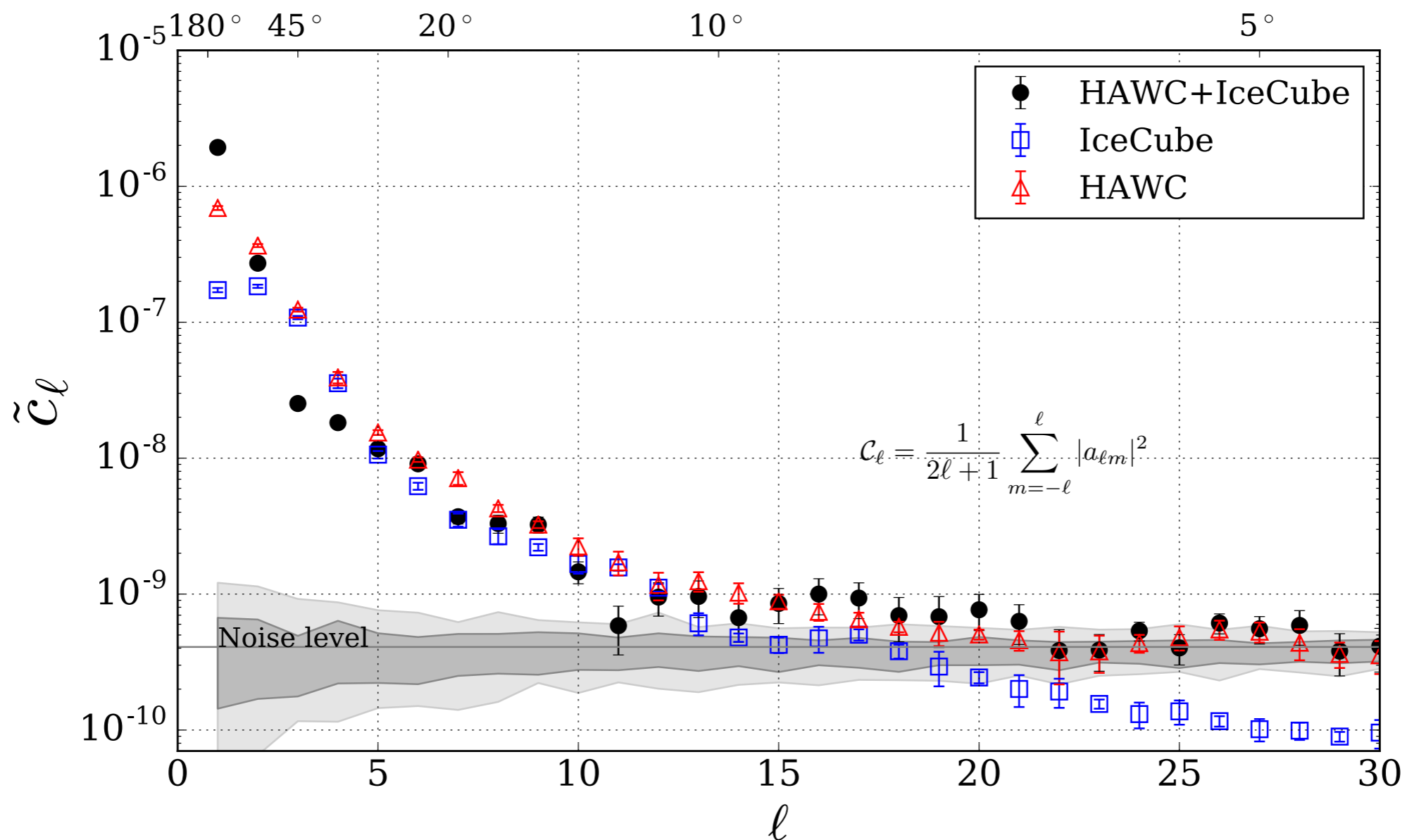
$$\delta_{0h} = 9.16e-4 \pm 4e-6$$

$$\delta_{6h} = 7.25e-4 \pm 4e-6$$

$\delta_{0h}$  and  $\delta_{6h}$  are the dipole components parallel to the equatorial plane and pointing to the direction of the local hour angle 0h ( $\alpha = 0^\circ$ ) and 6h ( $\alpha = 90^\circ$ ) of the vernal equinox, respectively. The dipole component pointing north  $\delta_N$  can not be constrained for ground-based observatories.



# Angular Power Spectrum



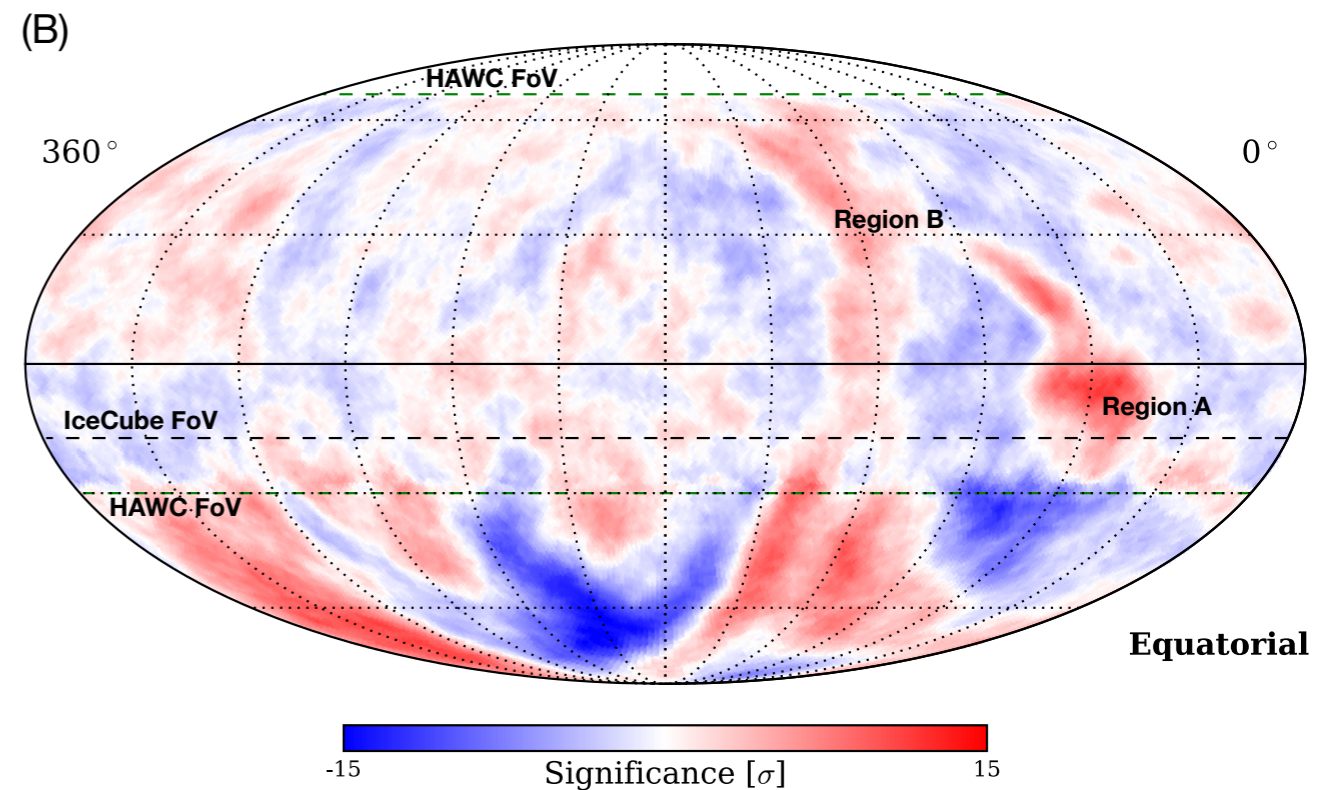
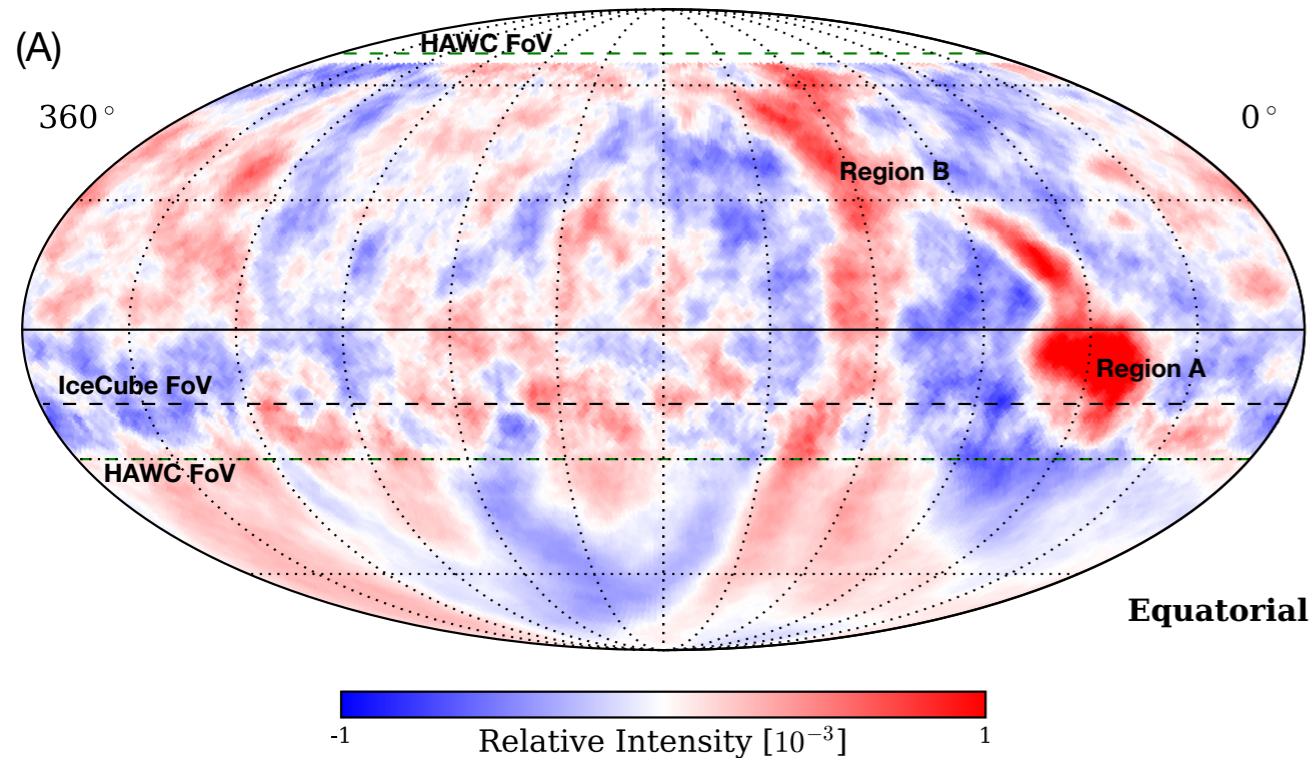
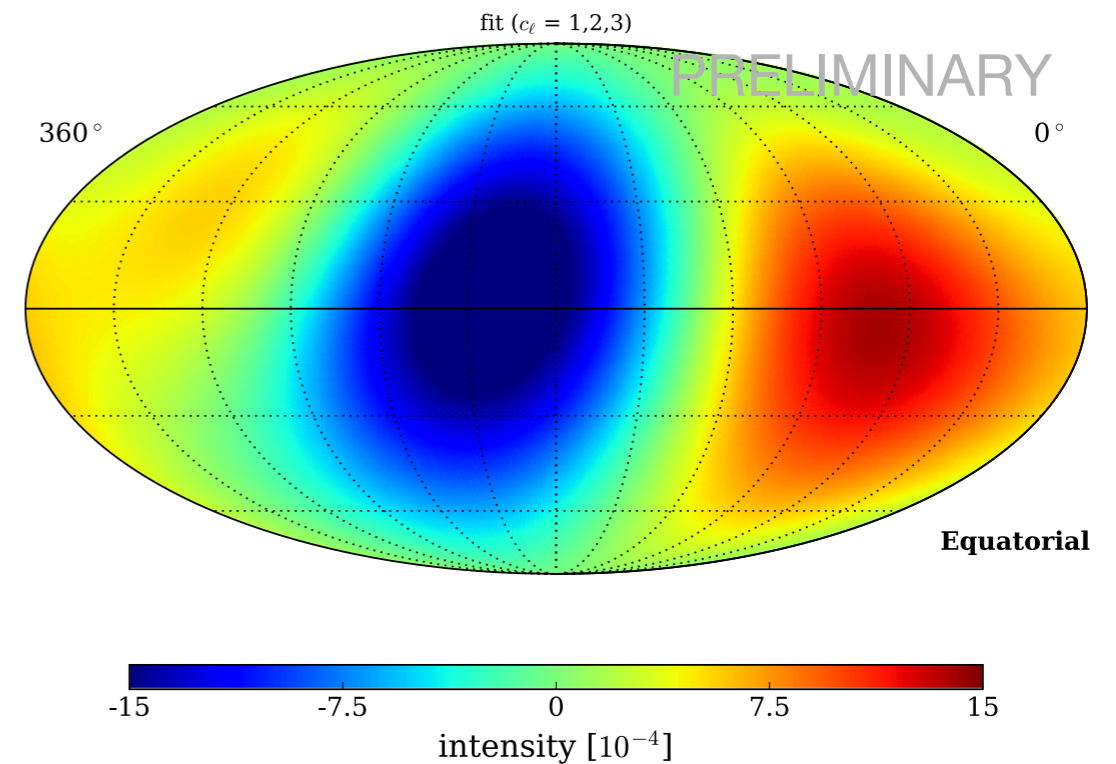
The angular pseudo-power spectrum of the cosmic ray anisotropy for the combined IceCube and HAWC dataset along with individual measurements. The dark and light gray band represent the power spectra for isotropic sky maps at the 68% and 90% confidence levels respectively. The structure appears to have a very steep spectrum at low  $\ell$  and a flatter spectrum at  $\ell > 3$ .

# Small-scale Anisotropy

Multipole fit

(A) We obtain the small-scale relative intensity by subtracting the multipole from the large-scale map.

(B) corresponding signed statistical significance  $S_i$  of the deviation from the average intensity in J2000 equatorial coordinates.





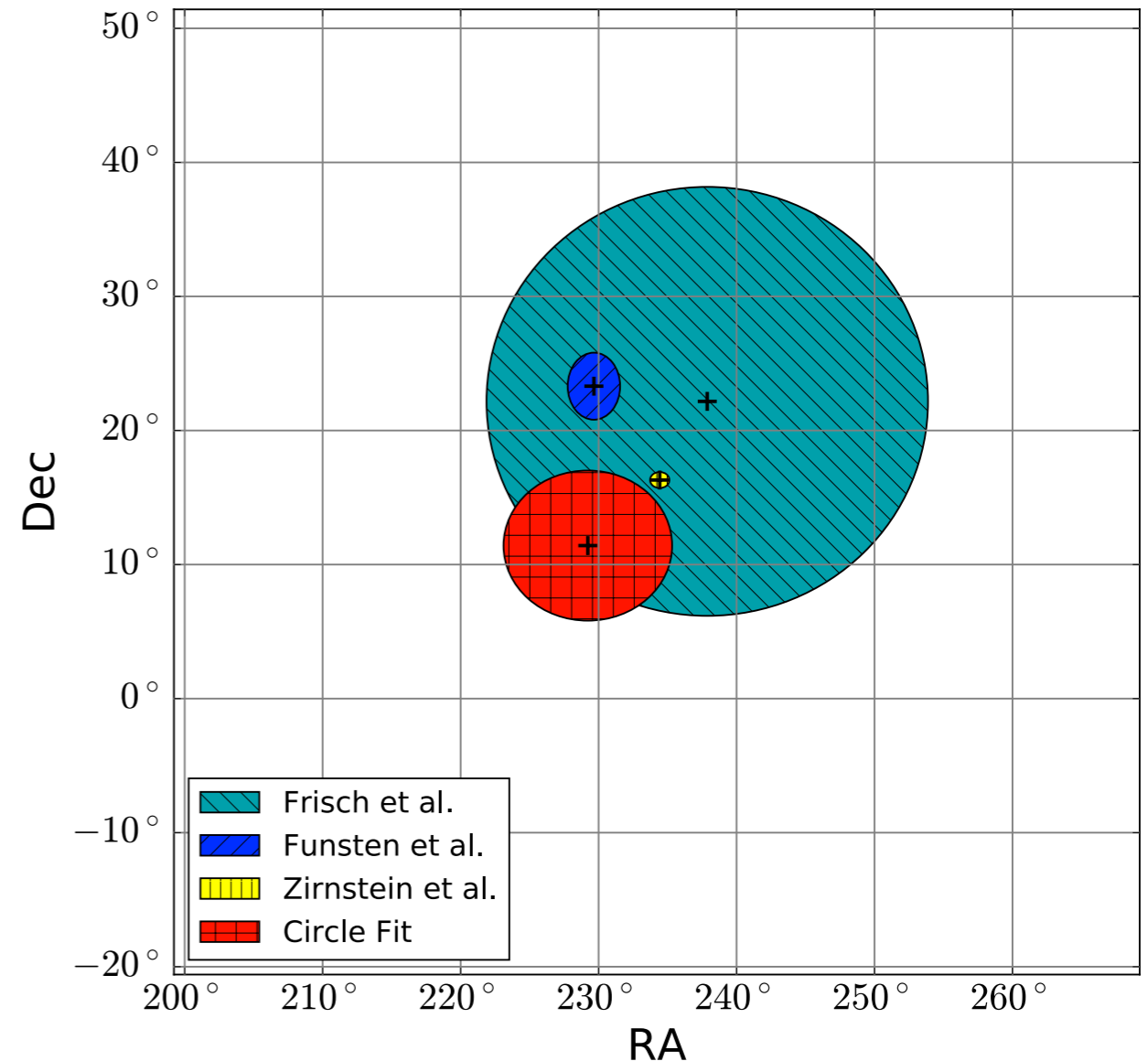
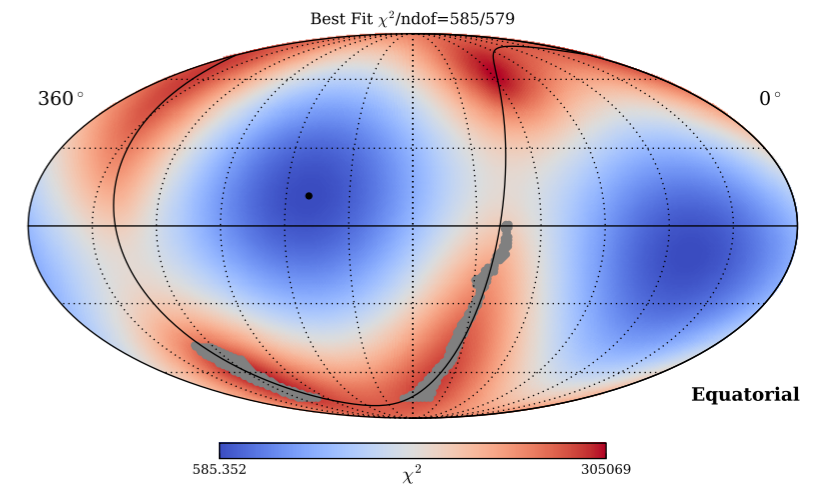
# Boundary alignment with LISM

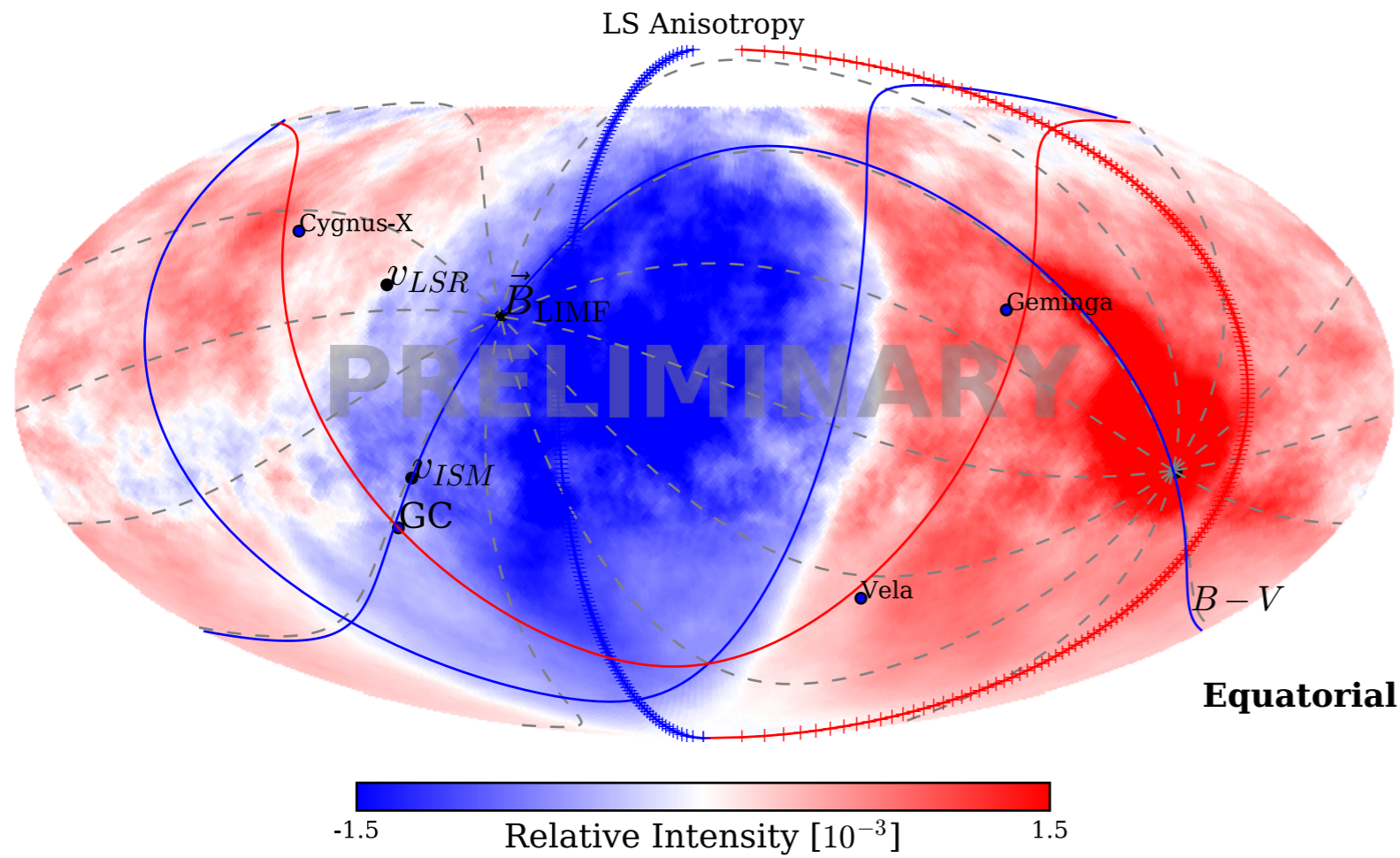
**A plane fit to the boundary between LS excess and deficit regions is approximately aligned with the direction of the LISM B-field from various studies.**

This provides a way to estimate the amplitude of the missing North-South dipole component amplitude of

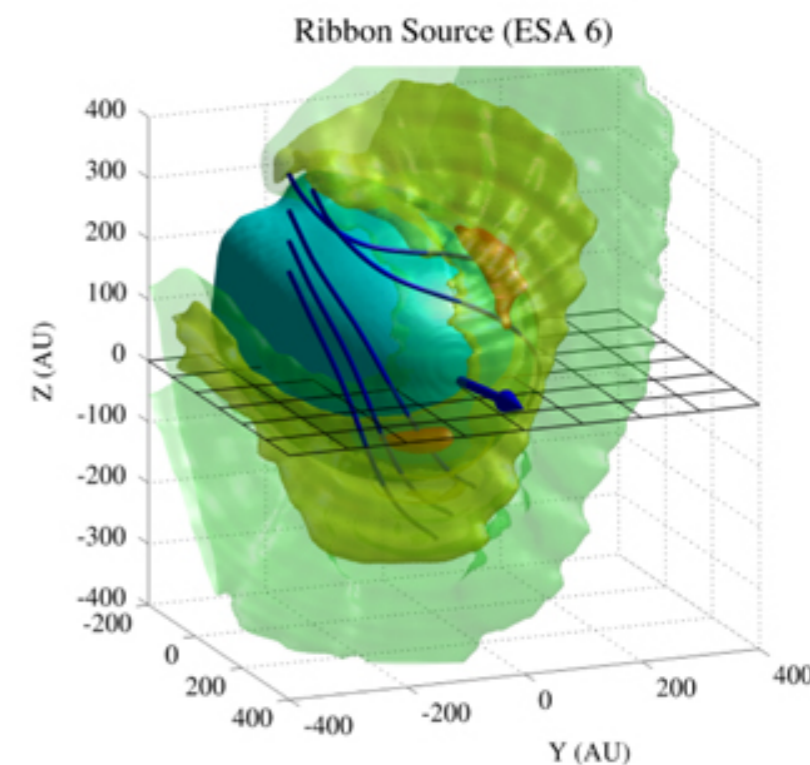
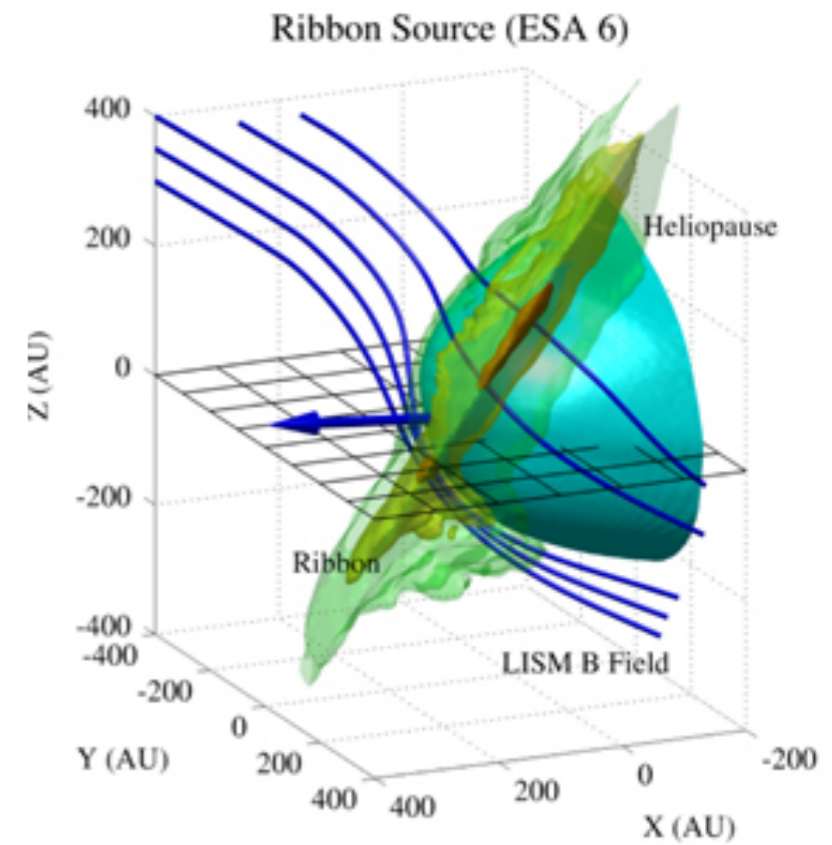
$$\delta_N \sim 3.97 (+1.0/-2.0) \times 10^{-4}$$

Source	R.A. [°]	decl [°]	$\Delta\Psi$ [°]	$\delta_N$ [10 <sup>-4</sup> ]
Funsten et al. (2013)	229.7 ± 1.9	23.3 ± 2.5	9.0	-5.03
Frisch et al. (2015)	237.9 ± 16	22.2 ± 16	12.2	-4.77
Zirnstern et al. (2016)	234.4 ± 0.7	16.3 ± 0.6	6.5	-3.42
Boundary Fit	229.2 ± 3.5	11.4 ± 3.0	-	-2.36
Dipole/Quadrupole	218.4 ± 0.3 (± 2.6)	20.7 ± 0.3 (± 2.6)	-	-4.41

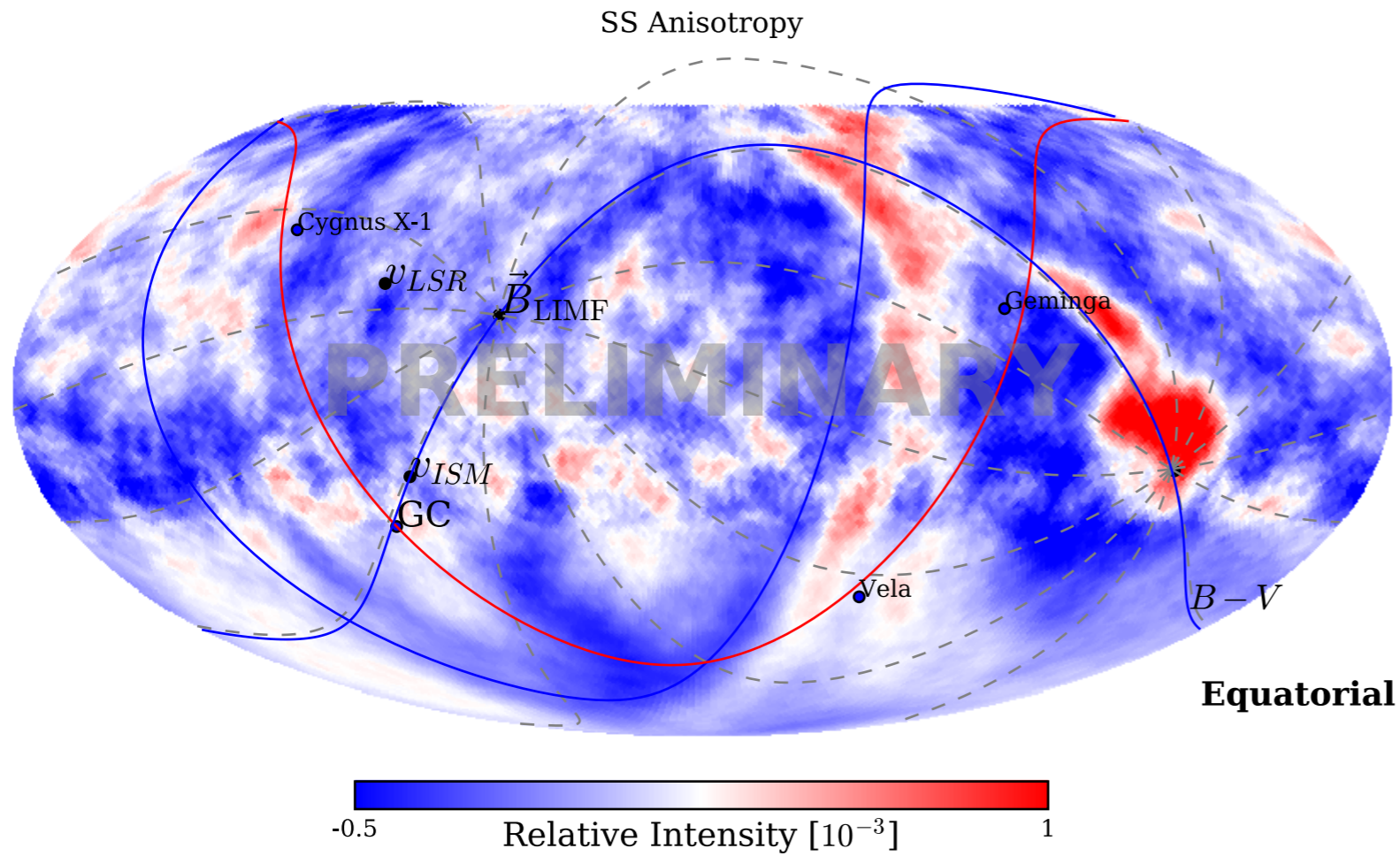




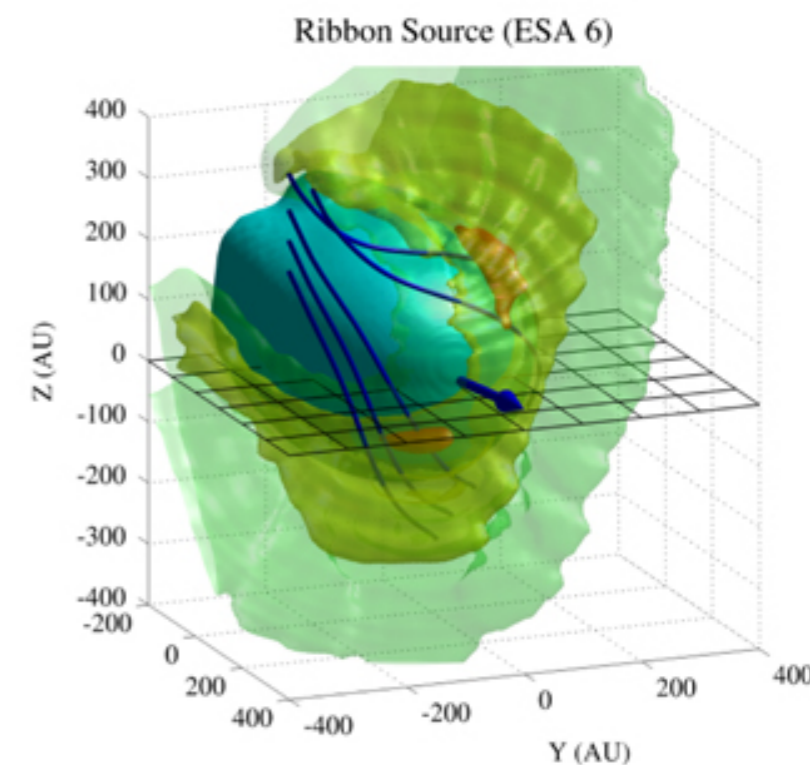
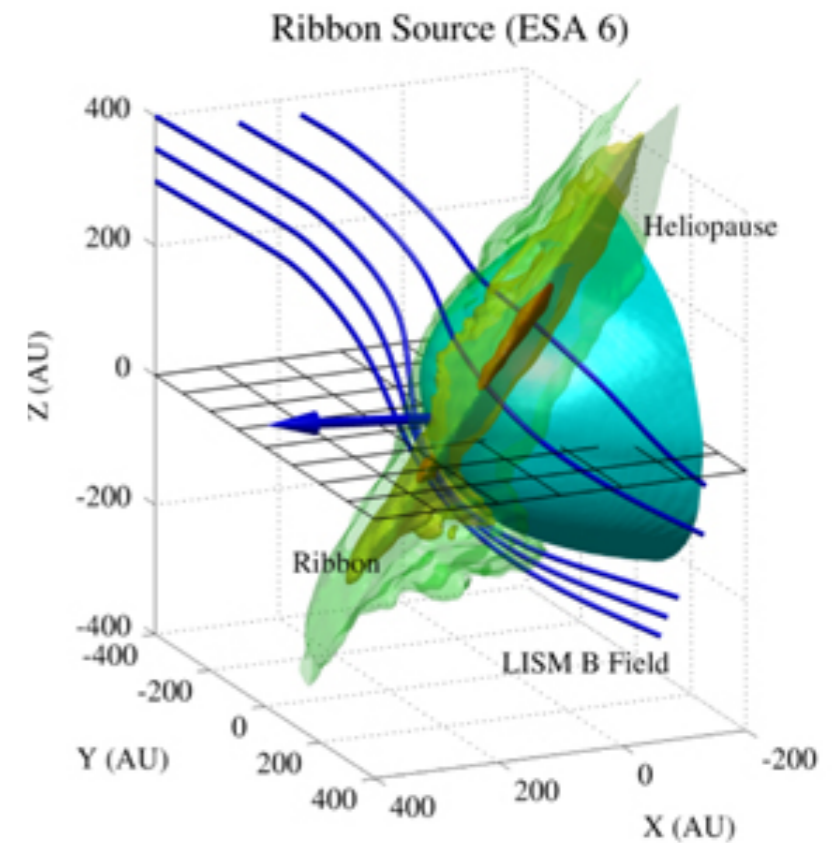
E. J. Zirnstien, et al. *ApJ Lett.* 2015



- Sharp boundary between excess and deficit regions is approximately aligned with the magnetic equator from the LIMF.
- Unlike dipole, boundary edge preserves directionality.



E. J. Zirnstern, et al. *ApJ Lett.* 2015



- Sharp boundary between excess and deficit regions is approximately aligned with the magnetic equator from the LIMF.
- Unlike dipole, boundary edge preserves directionality.
- Small-scale feature extending North from excess region "A" approximately follows B-V plane from -B

# Summary

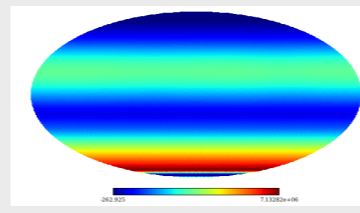
- This IceCube-HAWC study is the first (nearly) full-sky cosmic ray arrival direction distribution analysis with combined data from observatories in the North and South at the same primary energy of 10 TeV and is a key to probe into the origin of the CRA observations.
- Iterative maximum-likelihood reconstruction method simultaneously fits CR anisotropies and detector acceptance.
- Provides an optimal anisotropy reconstruction and the recovery of the dipole anisotropy for ground-based observatories located in middle latitudes.
- Ground-based observatories are generally insensitive to cosmic-ray anisotropy variations that are symmetric in RA, i.e. only vary across declination bands (i. e. dipole only observed as a projection onto celestial equator).
- Nearly full-sky coverage gives better fit of phase and amplitude of horizontal component of the dipole anisotropy.
- Significant small-scale structure is largely consistent with previous individual measurements.
- Small- and large-scale structures at 10 TeV appear to be qualitatively related with the local interstellar magnetic field and its interaction with the structure of the heliosphere.

# Backup

# Method for measuring CR anisotropy

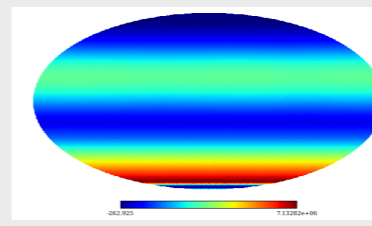
1

Build a binned data map using the equatorial coordinates of the events



2

Construct a “reference” map by integrating acceptance over 24 hours.

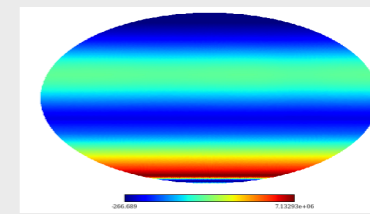


**Time-scrambling.**  $(\theta, \phi, t) \rightarrow (\alpha, \delta)$   
 $(\theta, \phi, t') \rightarrow (\alpha', \delta')$

**Direct integration.**  $\langle N(\alpha, \delta) \rangle = \int dt \int d\Omega A(ha, \delta) \cdot R(t) \cdot \epsilon(ha, \alpha, t)$

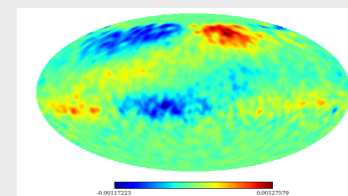
3

Correlate pixels to increase sensitivity to different angular scales



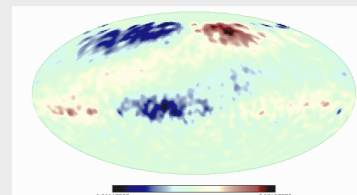
4

Calculate relative differences between data and reference with significance.



5

Calculate statistical significance for each pixel



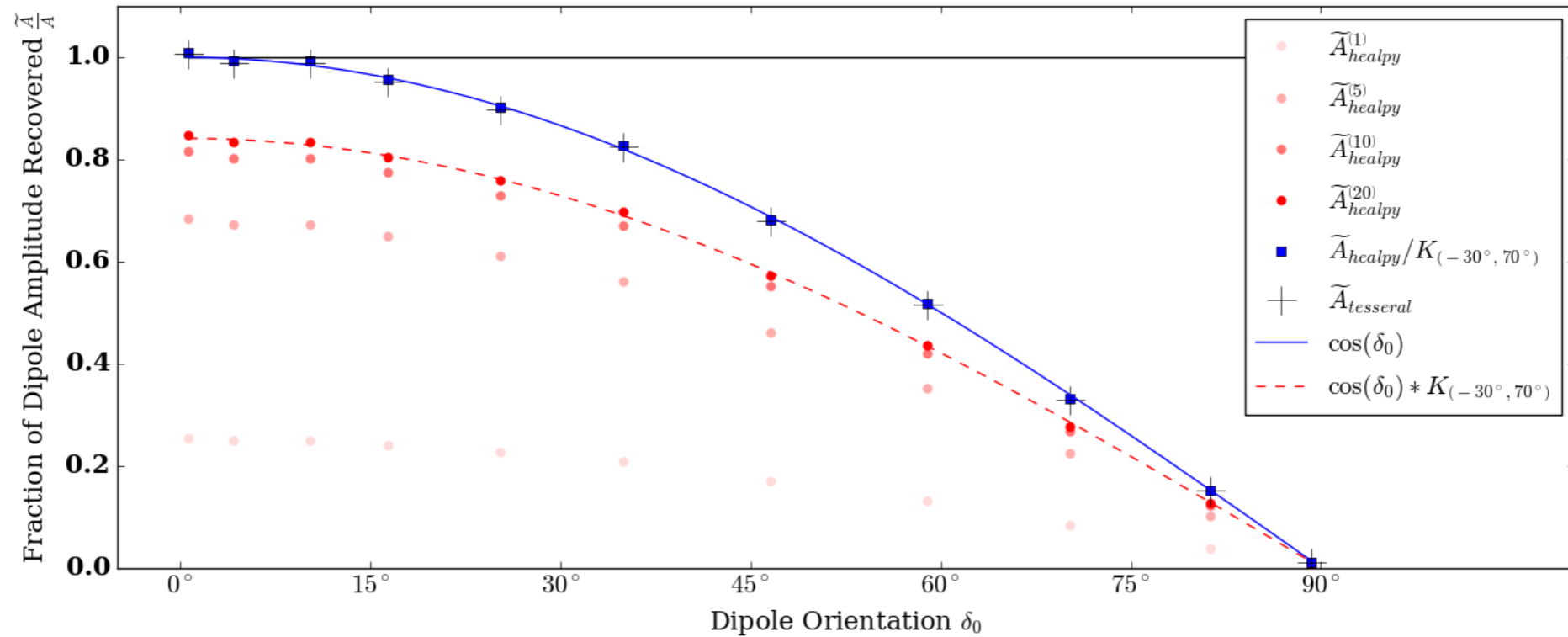
Relative Intensity

$$\delta I(\alpha, \delta)_i = \frac{N(\alpha, \delta)_i - \langle N \rangle(\alpha, \delta)_i}{\langle N \rangle(\alpha, \delta)_i}$$

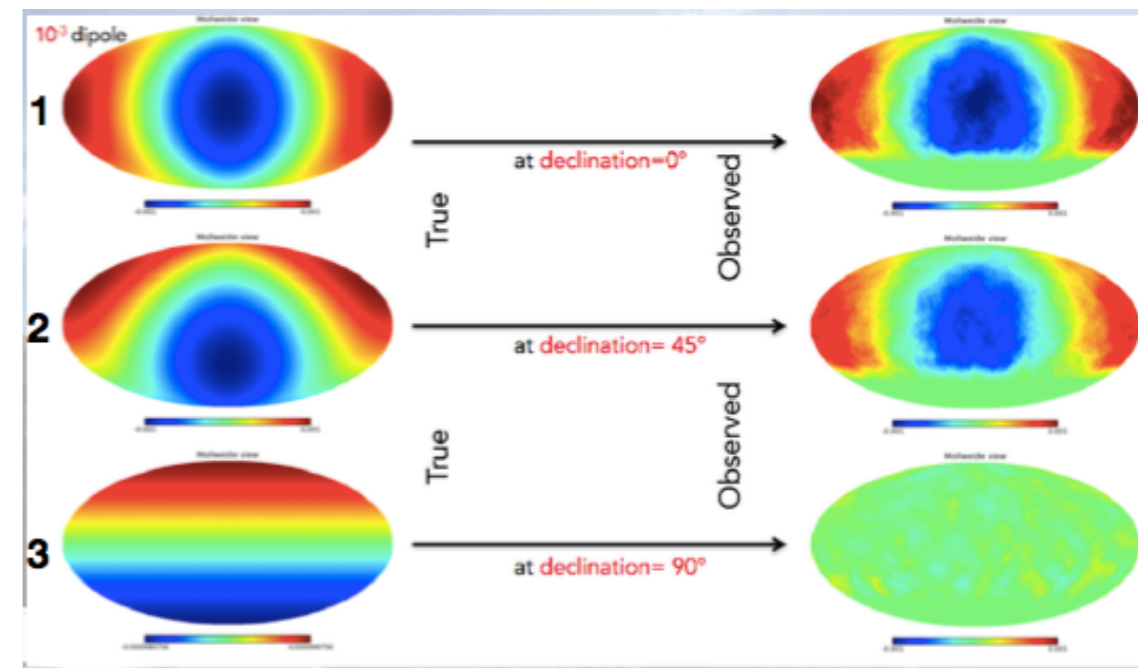
$$s_i = \sqrt{2} \left\{ N_i \log \left[ \frac{1 + \alpha}{\alpha} \left( \frac{N_i}{N_i + N_o} \right) \right] + N_o \log \left[ (1 + \alpha) \left( \frac{N_o}{N_i + N_o} \right) \right] \right\}^{1/2}$$

# Horizontal projection

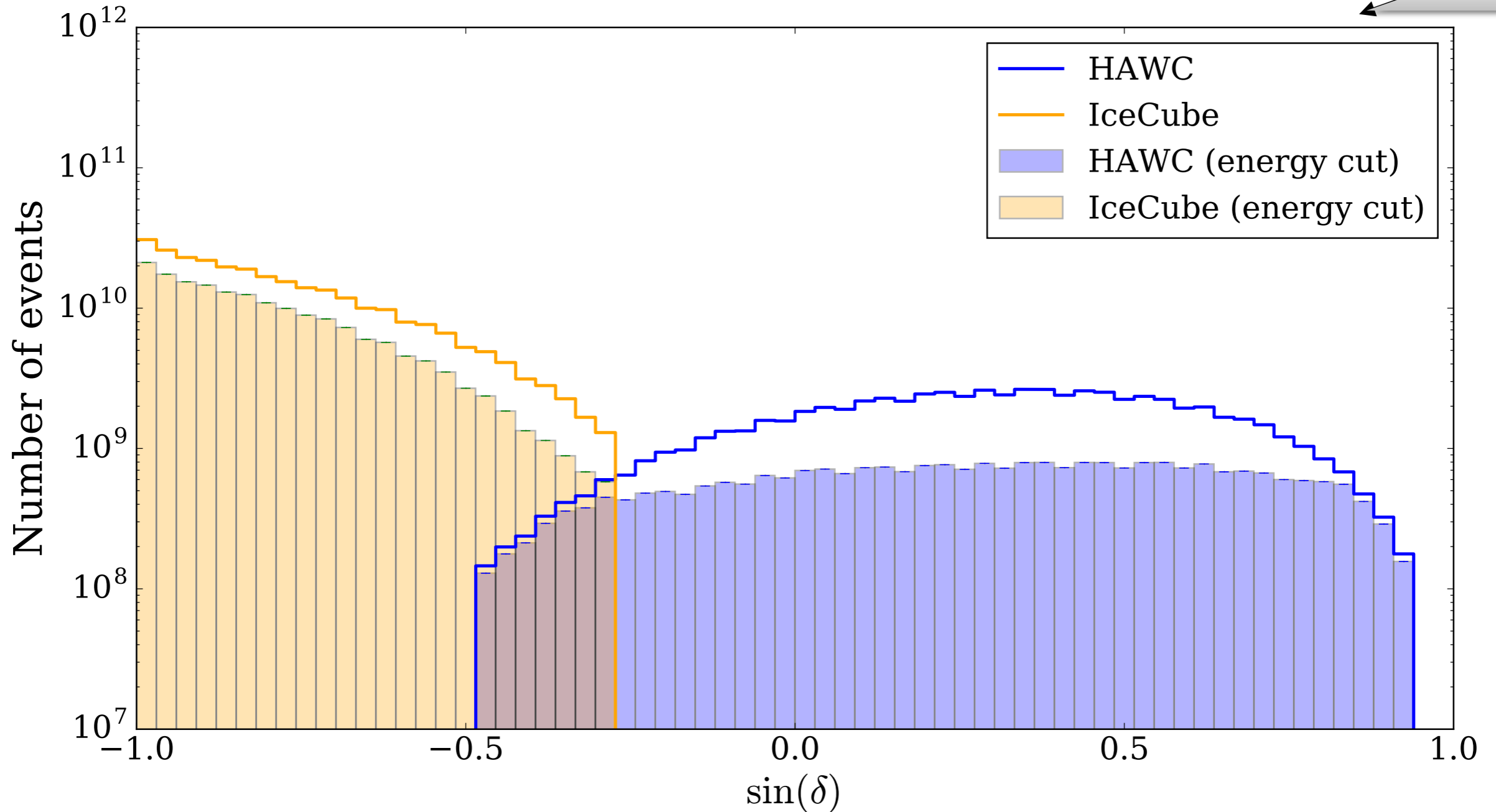
Pure dipole (reconstructed)



- Simulated dipole reconstructed with LLH method.
- Blue line is best possible with ground-based observations.
- Method improves with iteration (light to dark red).
- Geometric correction needed due to limited sky coverage.



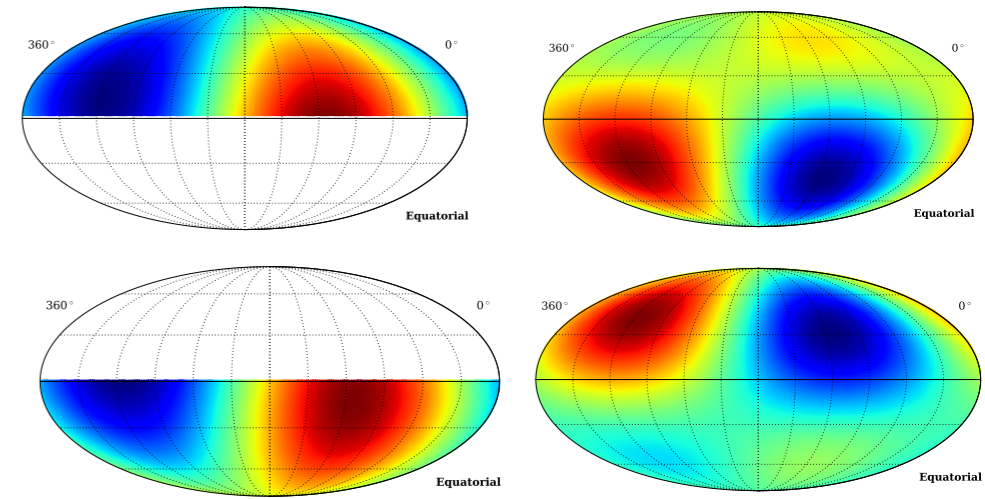
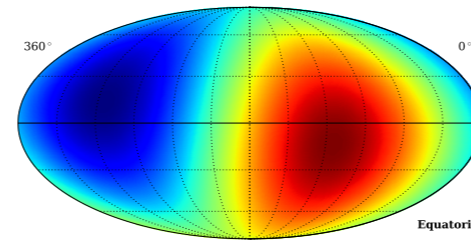
# The IceCube and HAWC Data Sets



Distribution of events as a function of declination for IceCube and HAWC. Triangles correspond to the full energy spectrum and squares correspond to the same datasets after applying energy cuts.



# Partial sky-coverage

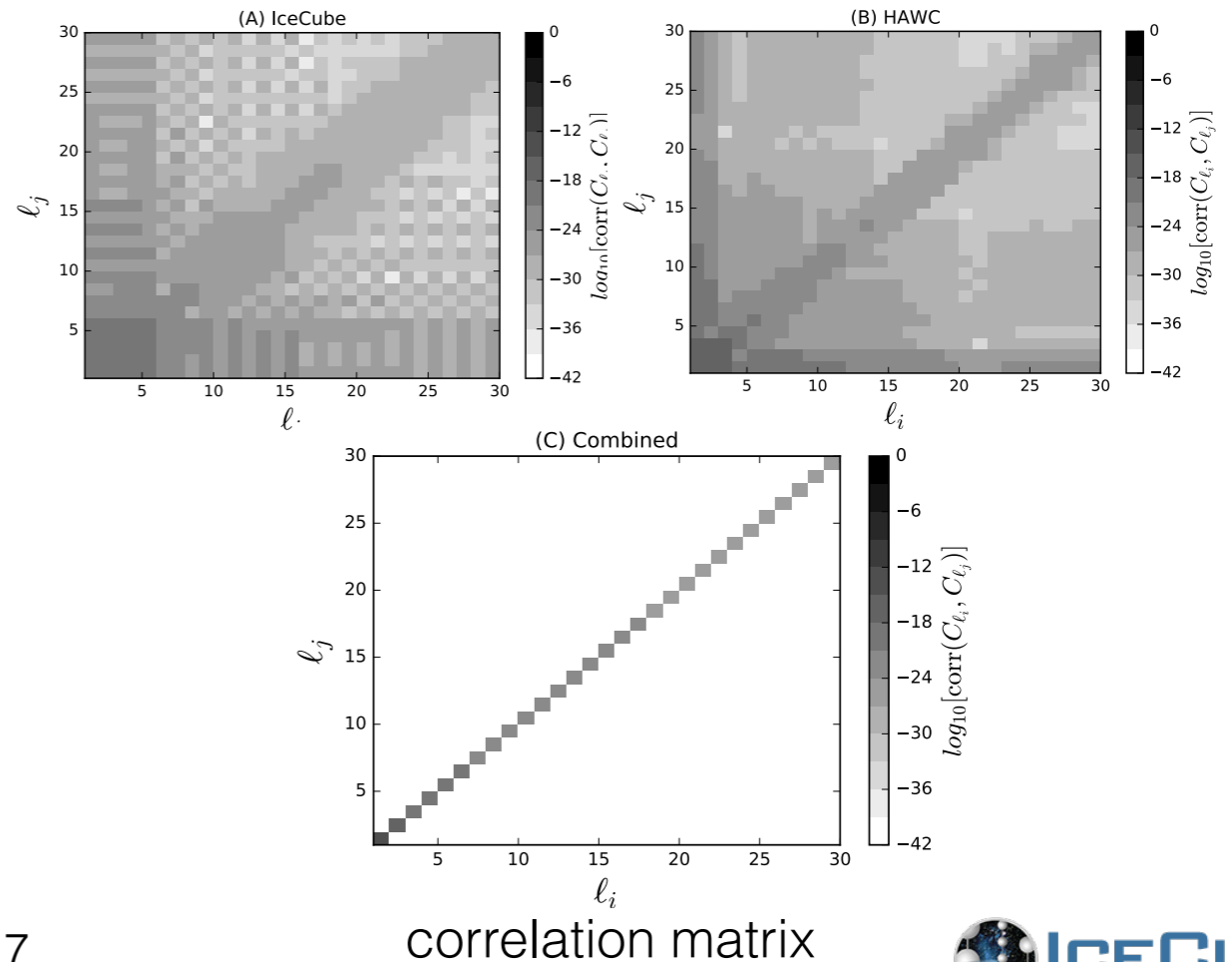
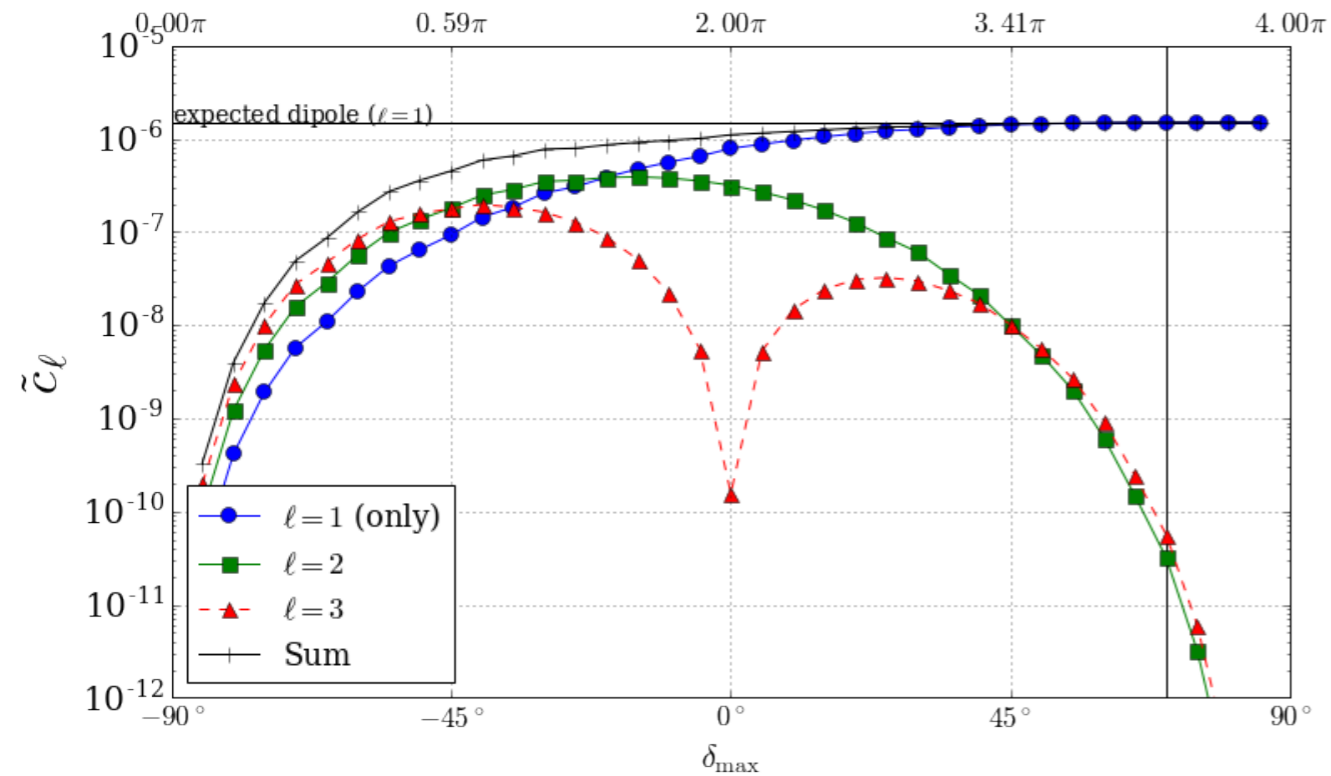


Multipole components are subject to correlations caused by partial sky coverage since there is a degeneracy between different  $\ell$ -modes.

Pure dipole (3d sensitivity)

A purely dipole can result in an artificial quadrupole due to partial sky coverage.

$$\delta_{6h}=0.0015, \delta_{0h}=0, \delta_N=0$$



correlation matrix

# The HAWC Observatory



Pico de Orizaba  
(Citlaltépetl)  
5636m

Sierra Negra  
4640m

Alfonso Serrano  
Large Millimeter  
Telescope

HAWC Site  
4100m



Pico de Orizaba



# The HAWC Observatory



## Mapping the Northern Sky in High-Energy Gamma Rays

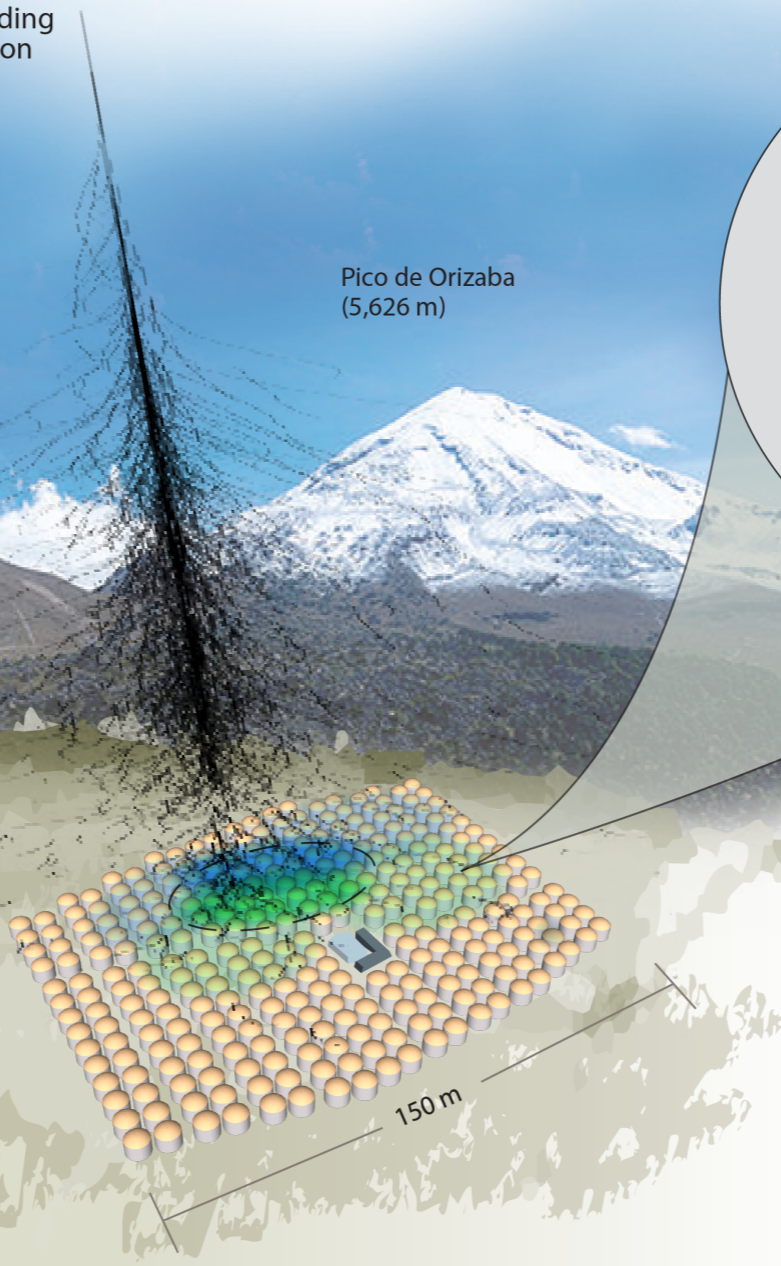
### HAWC Observatory

HAWC operates day and night, providing a large field of view for the observation of the highest energy gamma rays.



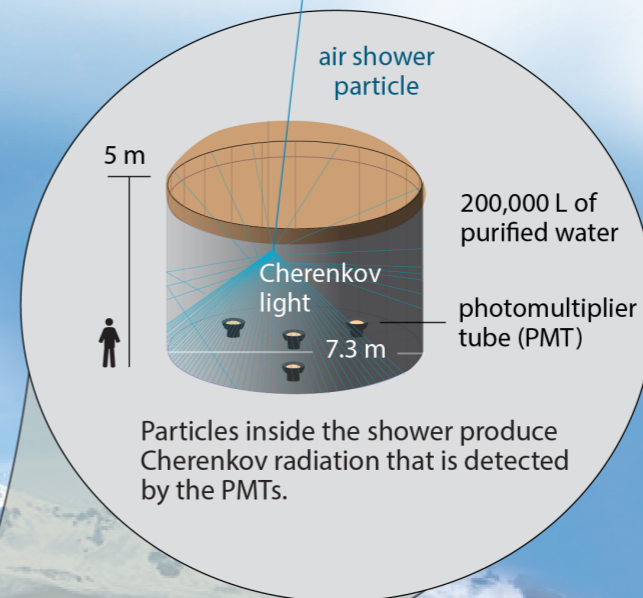
Pico de Orizaba  
(5,626 m)

HAWC is located at 4,100 m above sea level, covering an area of 20,000 m<sup>2</sup>.



### Water Cherenkov tank

HAWC comprises an array of 300 tanks that record the particles created in gamma-ray and cosmic-ray showers.

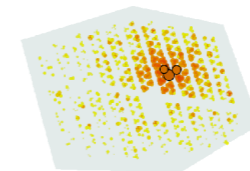


Particles inside the shower produce Cherenkov radiation that is detected by the PMTs.

### Gamma rays vs cosmic rays

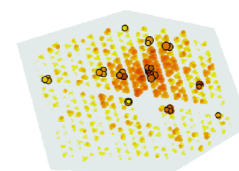
HAWC selects gamma rays from among a much more abundant background of cosmic rays.

gamma-ray shower



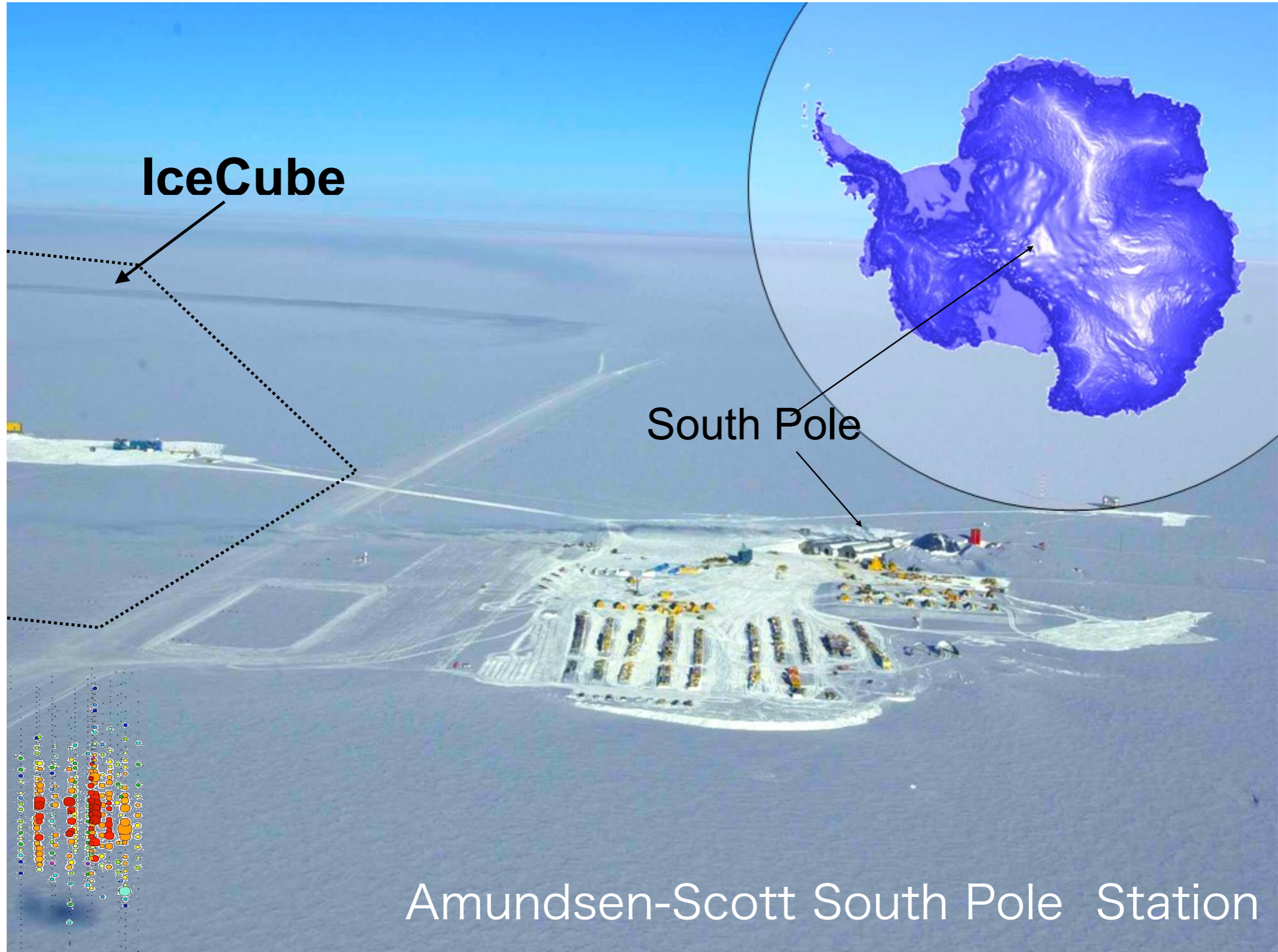
"hot" spots concentrate around the core

cosmic-ray shower

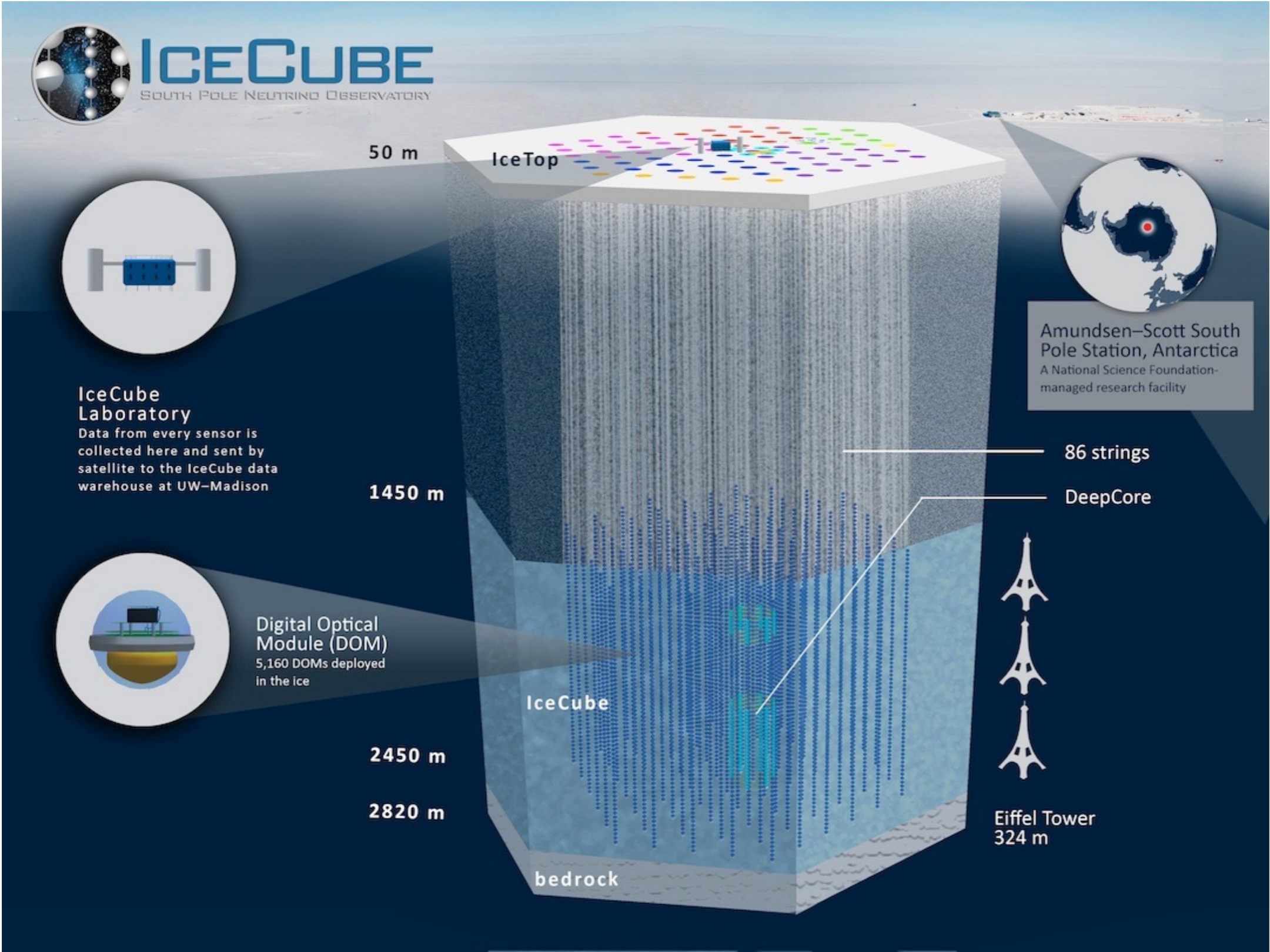


"hot" spots are more dispersed

# The IceCube Observatory



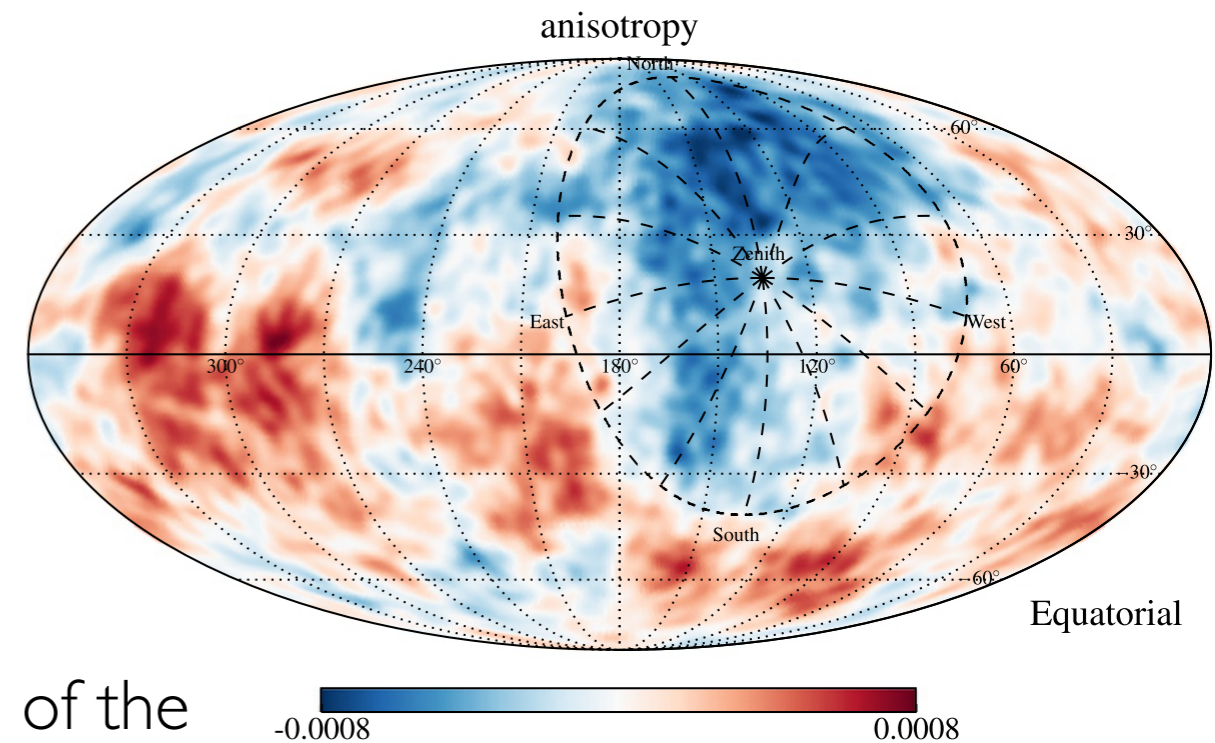
# The IceCube Observatory



# Iterative maximum likelihood method

Ahlers, BenZvi, Desiati, Díaz-Vélez, Fiorino, Westerhoff (arXiv.1601.07877)

- Traditional time-integration methods can strongly attenuate large-scale structures exceeding the size of the instantaneous field of view for detectors located at mid latitudes.
- A fixed position on the celestial sphere is only observable over a limited period every day. The total number of cosmic ray events from a fixed position can only be compared against reference data observed during the same period.
- This can lead to an under- or overestimation of the isotropic reference level.



M. Ahlers et al (arXiv.1601.07877)

# Iterative maximum likelihood method

Ahlers, BenZvi, Desiati, Díaz-Vélez, Fiorino, Westerhoff (arXiv.1601.07877)

The likelihood of observing  $n$  cosmic rays is given by the product of Poisson probabilities

$$\mathcal{L}(n|I, \mathcal{N}, \mathcal{A}) = \prod_{\tau i} \frac{(\mu_{\tau i})^{n_{\tau i}} e^{-\mu_{\tau i}}}{n_{\tau i}!},$$

Maximize the likelihood ratio via null hypothesis in  $N, A$  y  $I$

$$\lambda = \frac{\mathcal{L}(n|I, \mathcal{N}, \mathcal{A})}{\mathcal{L}(n|I^{(0)}, \mathcal{N}^{(0)}, \mathcal{A}^{(0)})}$$

maximum values  $(I^*, N^*, A^*)$  must follow

$$I_a^* = \sum_{\tau} n_{\tau a} / \sum_{\kappa} \mathcal{A}_{\kappa a}^* \mathcal{N}_{\kappa}^*,$$

$$\mathcal{N}_{\tau}^* = \sum_i n_{\tau i} / \sum_j \mathcal{A}_j^* I_{\tau j}^*,$$

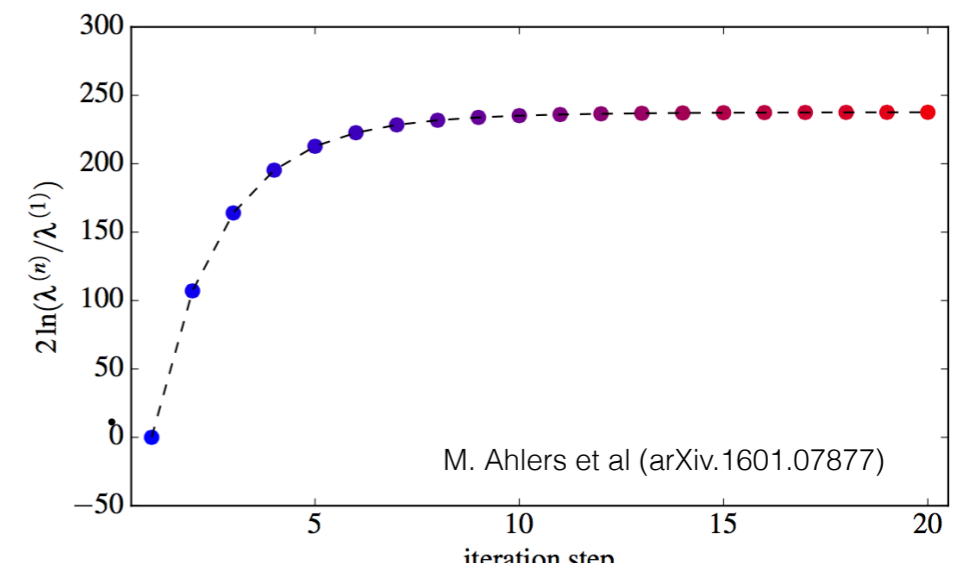
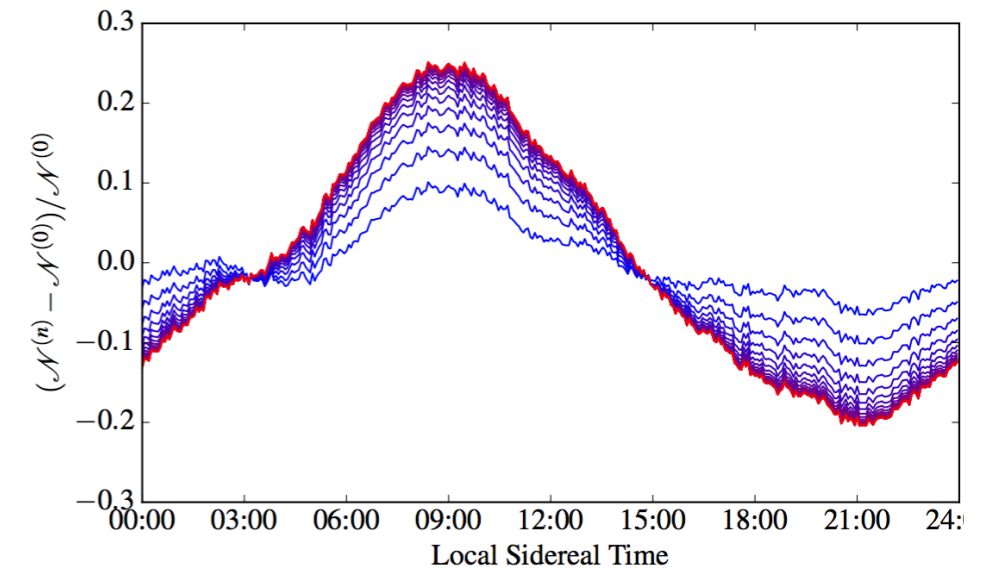
$$\mathcal{A}_i^* = \sum_{\tau} n_{\tau i} / \sum_{\kappa} \mathcal{N}_{\kappa}^* I_{\kappa i}^*,$$

which can be solved iteratively.

relative intensity  $\downarrow$  relative acceptance  $\swarrow$

$$\mu_{\tau i} \simeq I_{\tau i} \mathcal{N}_{\tau} \mathcal{A}_i$$

$\uparrow$   
expected number of events from isotropic background



M. Ahlers et al (arXiv.1601.07877)

# Compton-Getting

Not from movement of Sun around Galactic center but through ISM

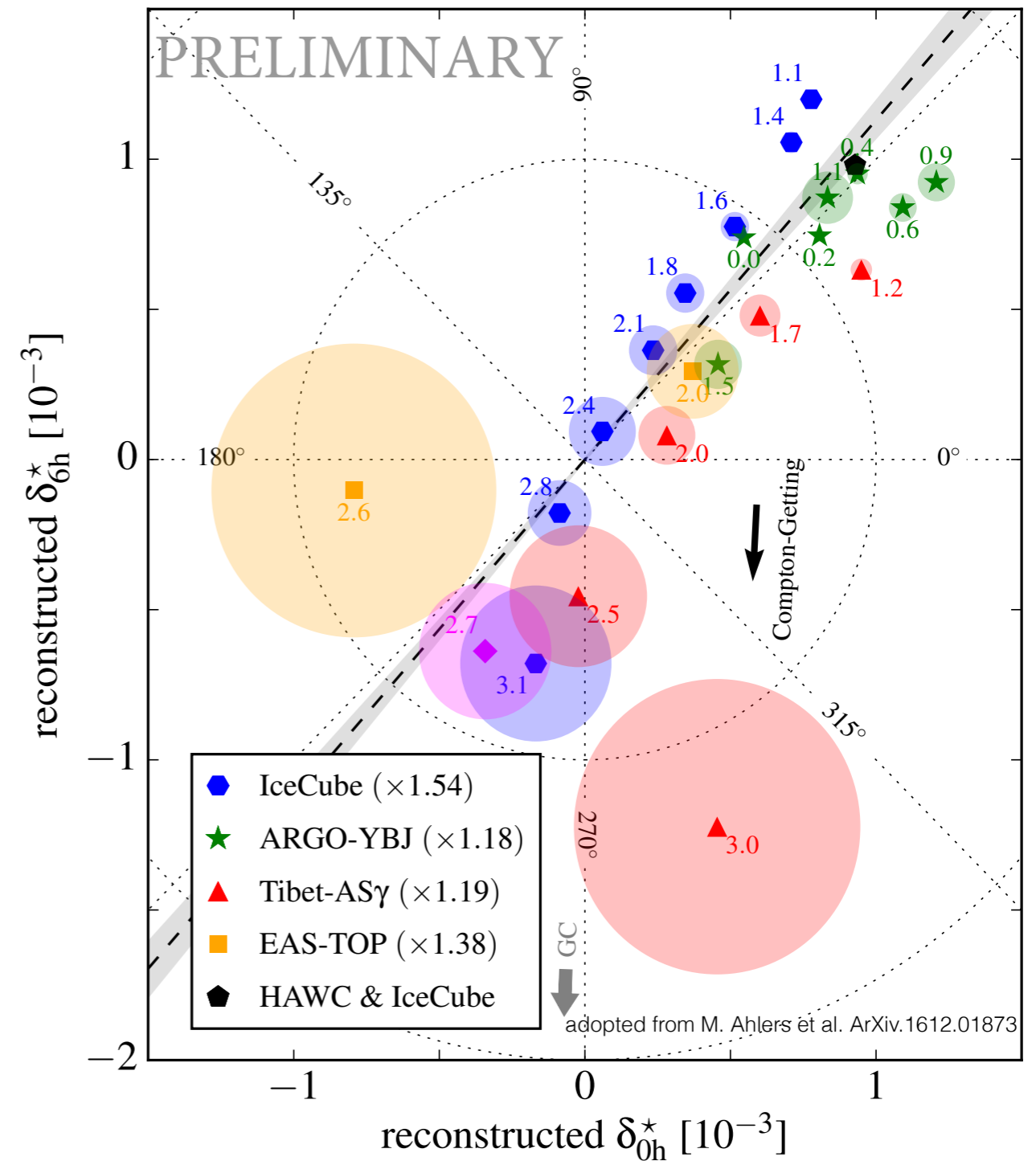
$$v_{\text{ISM}} \approx 23.2 \text{ km/s in towards } (l \approx 5.25^\circ, b \approx 12.0^\circ)$$

McComas et al. Science 336 (2012) 1291

Phase diagram in polar coordinates.

The amplitude corresponds to the radial distance while the phase corresponds to the angle in the counter-clockwise direction of the x-axis.

The values calculated in the figure take into account and subtract the contribution of the Compton-Getting effect which is estimated at a magnitude of  $4.5 \times 10^{-4}$  and pointing in the direction of 6h.



C-G corrected values.

$$A_1 = 1.35e-3$$

$$\alpha_1 = 46.6^\circ$$

$$\delta_{0h} = 0.929e-3$$

$$\delta_{6h} = 0.979e-3$$





# Origin of anisotropy

## Distribution of CR sources

A number of theories have proposed scenarios where the large-scale anisotropy results from the distribution of cosmic ray sources in the Galaxy and of their diffusive propagation

### Diffusive propagation from distribution of cosmic ray sources

A. D. Erlykin and A. W. Wolfendale, *Astropart. Phys.* 25 (2006) 183–194.

P. Blasi and E. Amato, *JCAP* 1 (2012) 11.

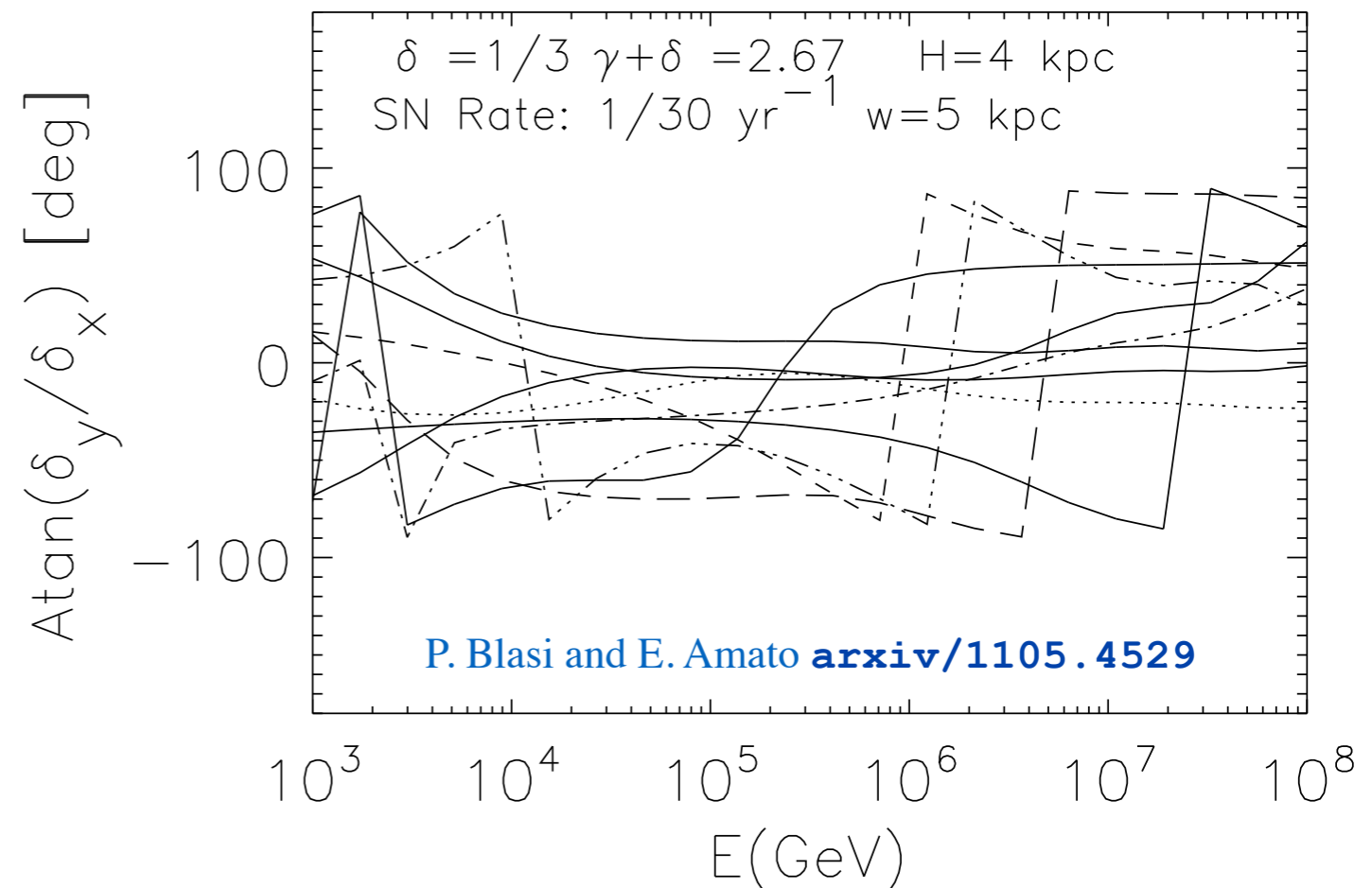
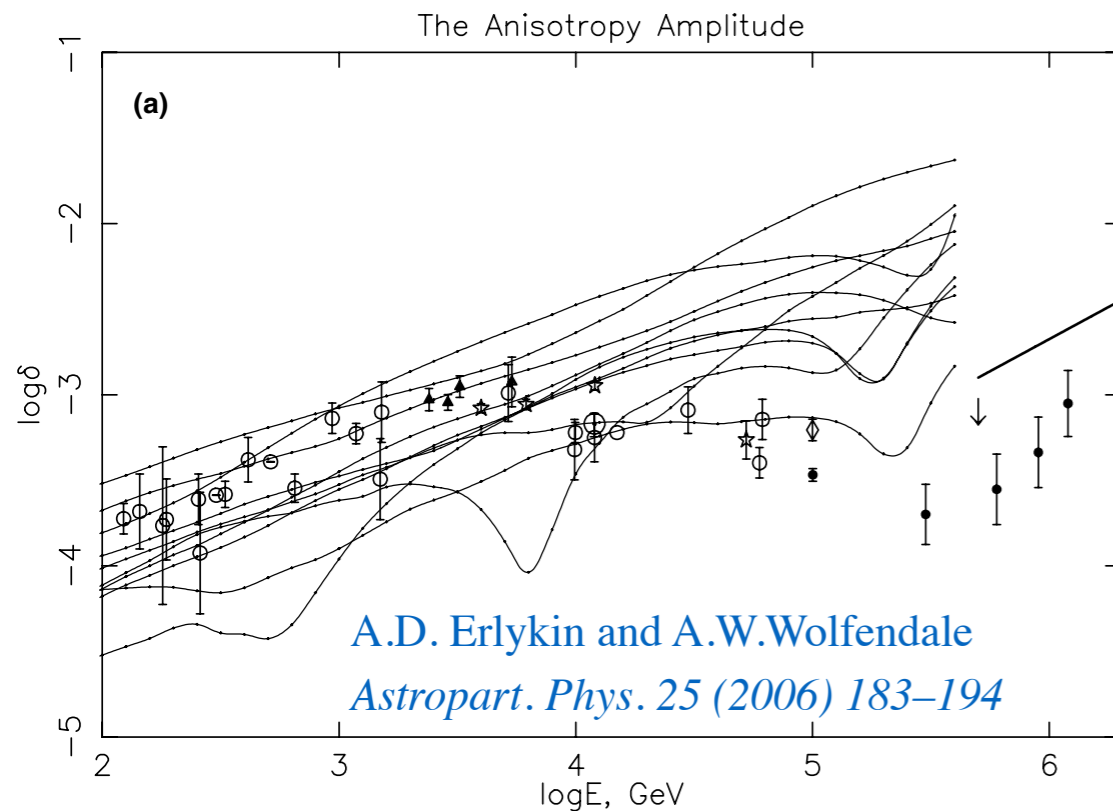
V. Ptuskin, *Astropart. Phys.* 39 (2012) 44–51.

M. Pohl and D. Eichler, *Astrophys. J.* 766 (2013) 4.

L. G. Sveshnikova, et al. *Astropart. Phys.* 50 (2013) 33–46.

R. Kumar and D. Eichler, *Astrophys. J.* 785 (2014) 129.

P. Mertsch and S. Funk, *Phys. Rev. Lett.* 114 (2015) 021101.



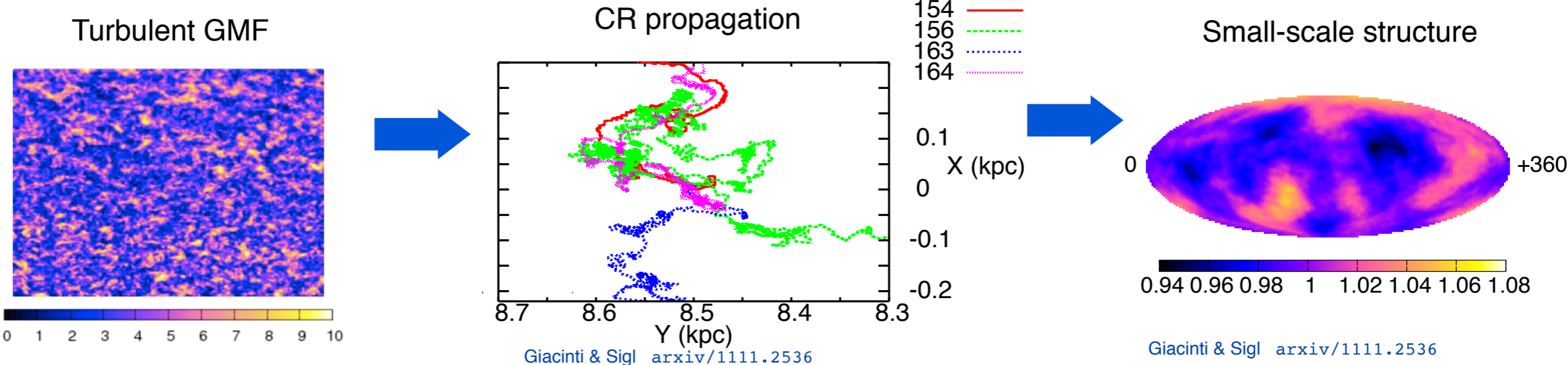
# Origin of small-scale anisotropy

It is expected that cosmic rays should lose any correlation with their original direction due to diffusion as they traverse through interstellar magnetic fields.

## Propagation effects in ISMF

Giacinti & Sigl, Phys. Rev. Lett. 109, 071101 (2012)

López-Barquero, et al, ApJ 830 19 (2016)

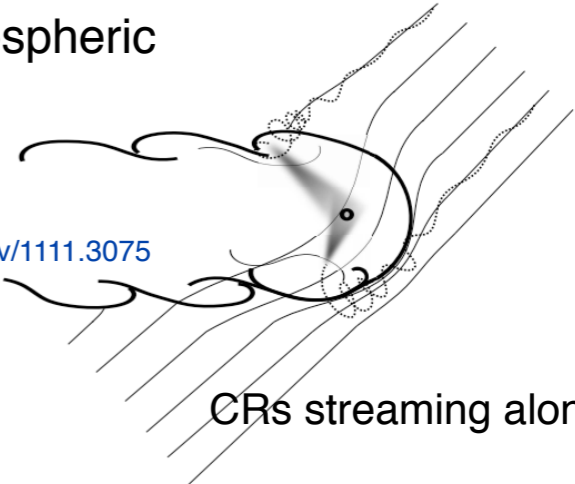


## Heliospheric effects

Desiati and Lazarian, ApJ, 762, 1 (2013)  
 Pogorelov et al., ApJ772 (2013) 2  
 M. Zhang, et al, Astrophys. J. 790 (2014) 5  
 López-Barquero, et al ApJ, 842, 54 (2017)

Ripples in heliospheric boundary

Desiati & Lazarian arxiv/1111.3075

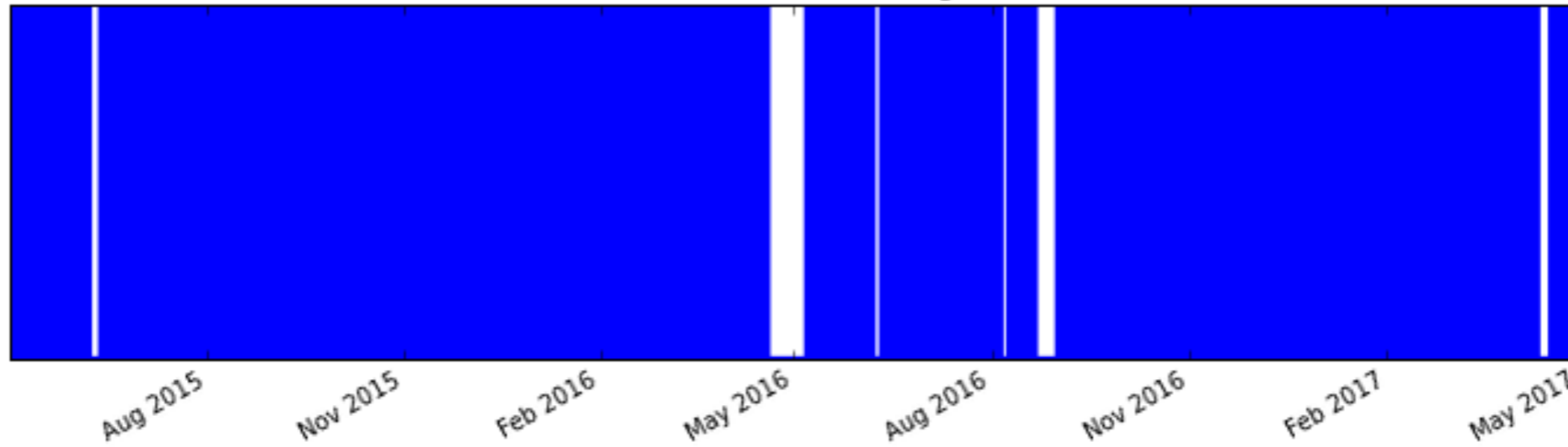


CR scattering on ripples in the heliosphere boundary induce small-scale anisotropy.

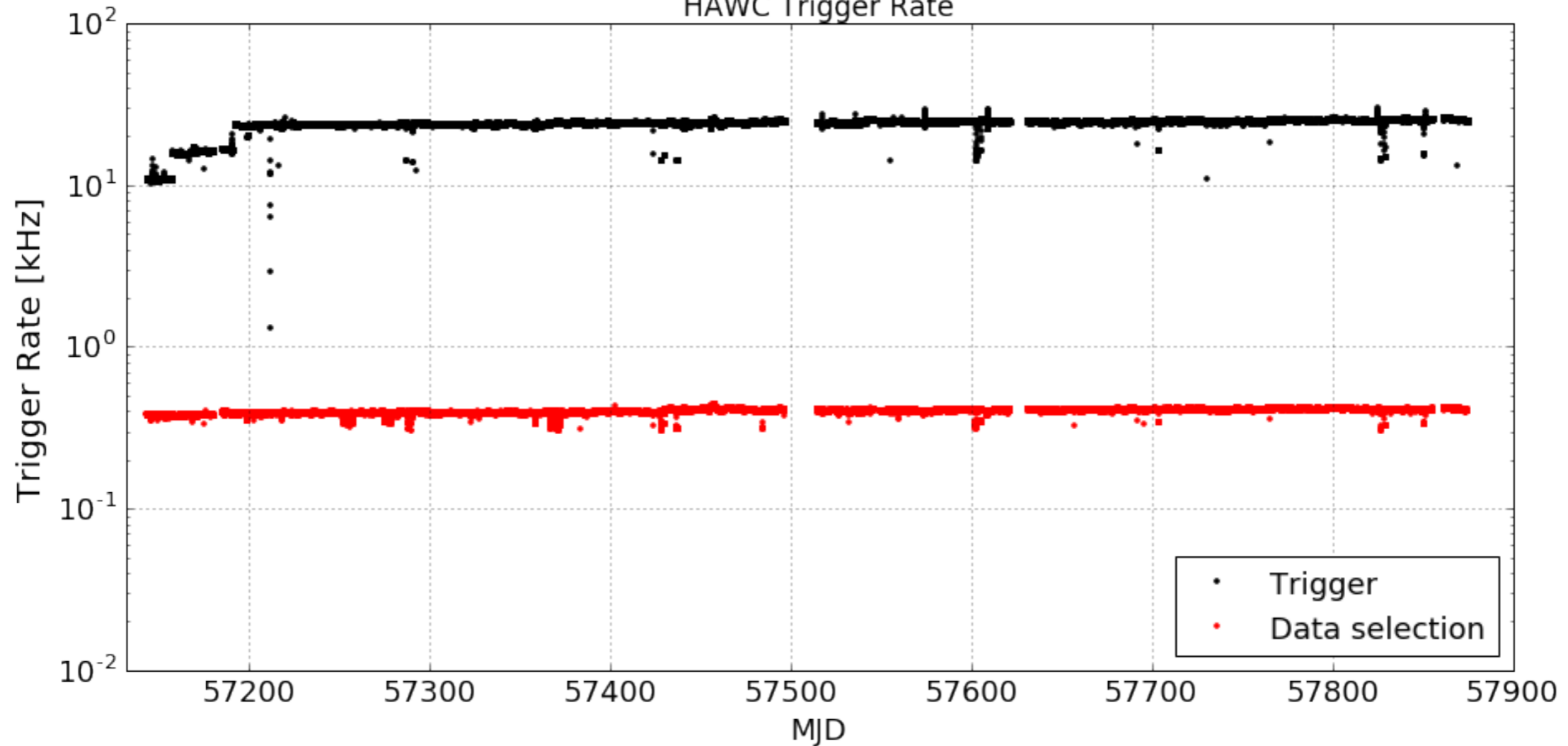
CRs streaming along LIMF

# HAWC Data Coverage

HAWC300 data coverage

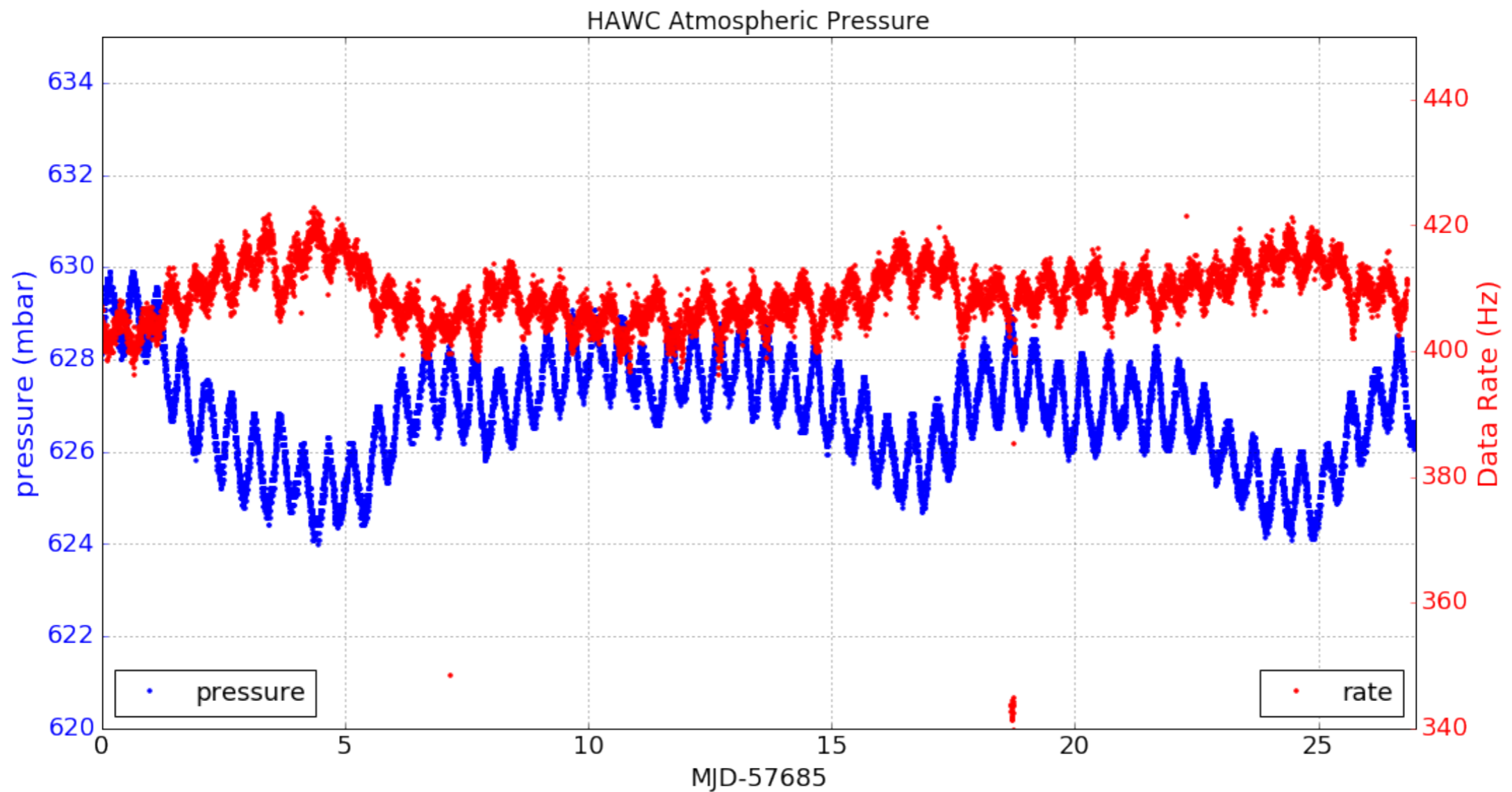


HAWC Trigger Rate



# Atmospheric tides.

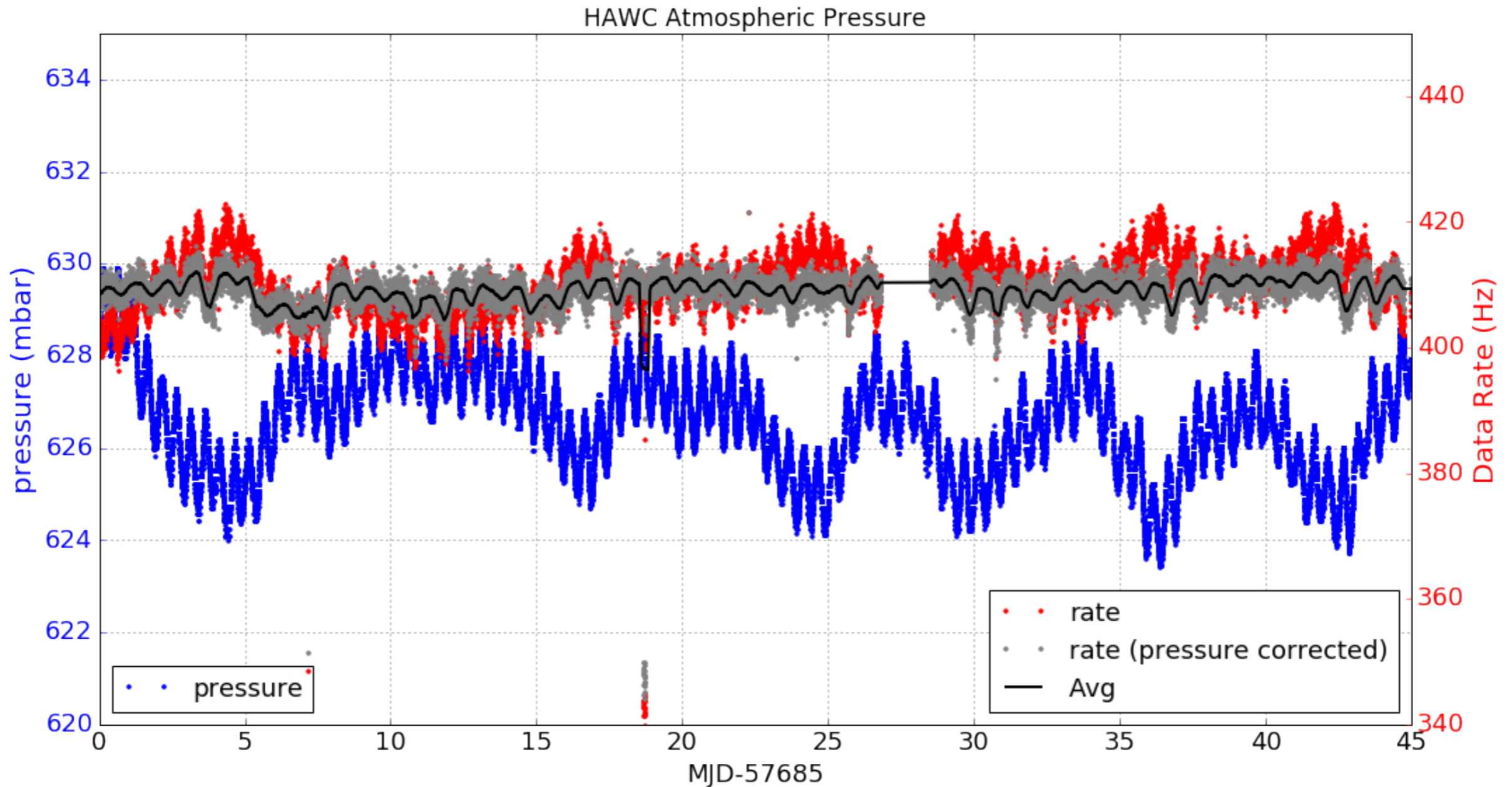
- Lunar or gravitational tides.
- Thermally driven tides. heating associated with solar radiation. Dynamics determined by both the Coriolis force and gravity. (X. Zhang, et a. J. Geoph. Res.. Space Physics)



# Atmospheric pressure correction

Atmospheric tides.

- Lunar gravitational tides.
- Thermally driven tides. heating associated with solar radiation. Dynamics determined by both the Coriolis force and gravity. (X. Zhang, et al. J. Geoph. Res., Space Physics (2010))

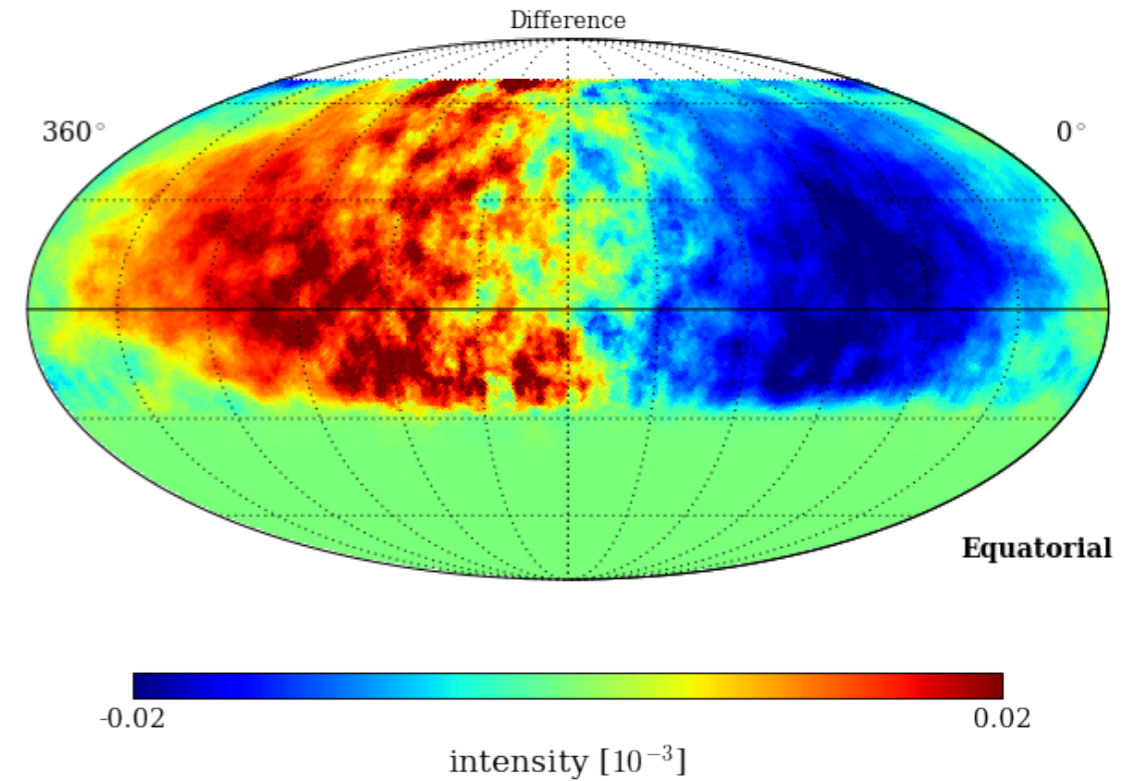


# Solar dipole correction (HAWC)

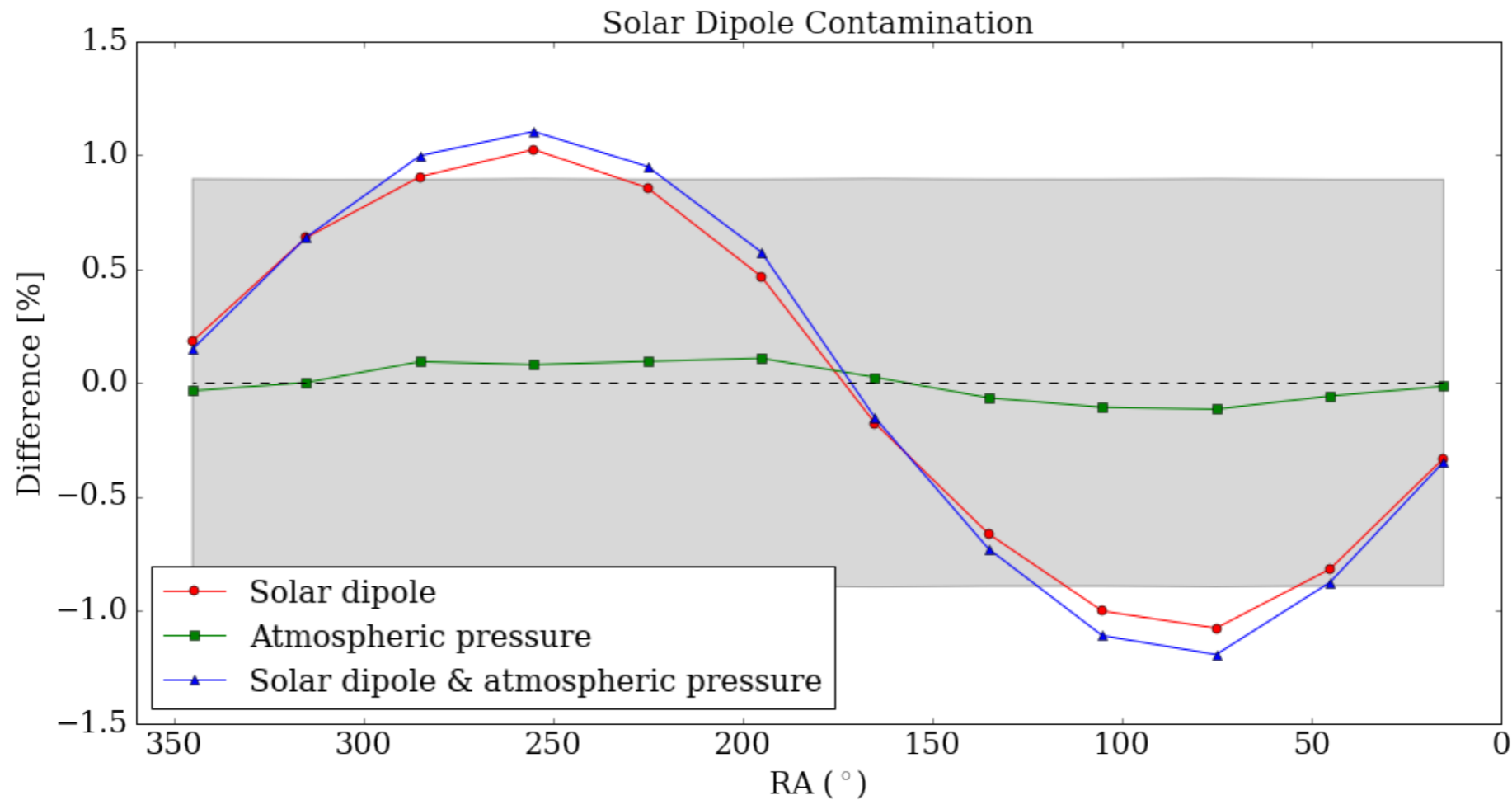
Relative movement of the Earth in the solar system

$$\frac{\Delta I}{\langle I \rangle} = (\gamma + 2) \frac{v}{c} \cos(\theta_v)$$

A weight is added to each event to correct the solar dipole and atmospheric variations.

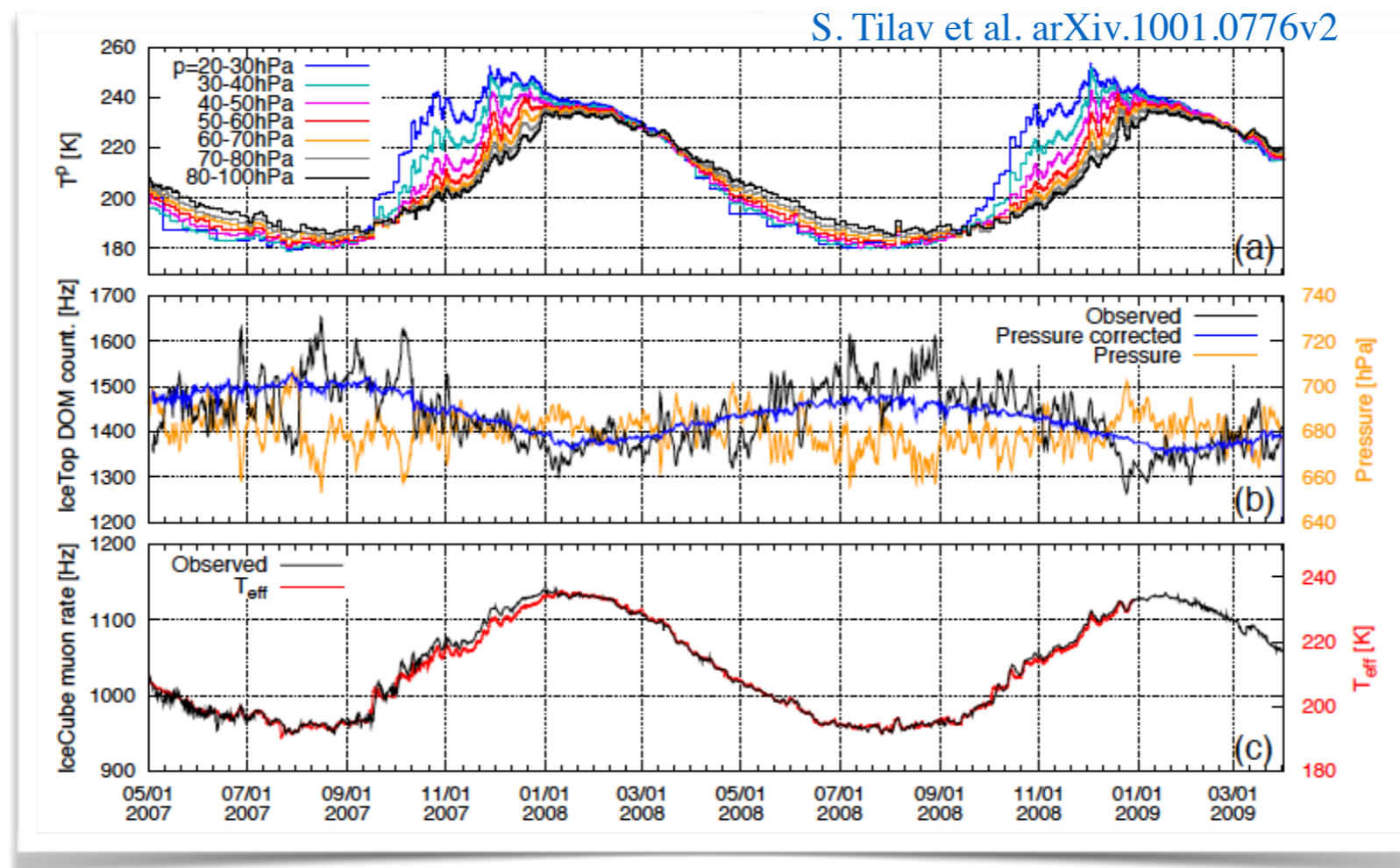


The difference is small compared to statistical errors.

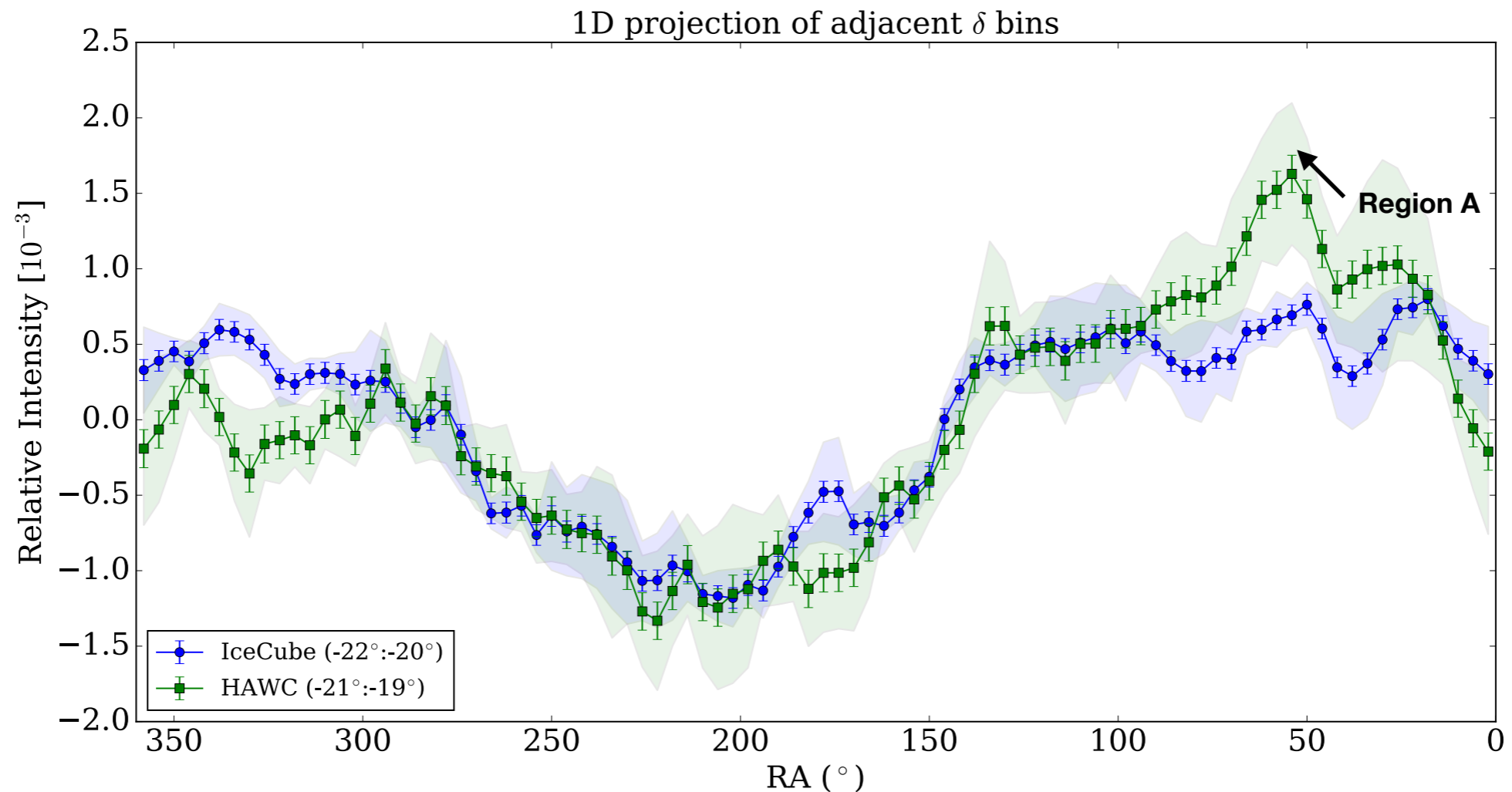


# Seasonal variations in IceCube

- Modulations in IceCube trigger rates have an annual period since the solar cycle in the South Pole has 365 days instead of 24 hours.
- In IceCube there are also atmospheric variations of higher frequency (and lower amplitude) but these affect the event rate simultaneously in all directions of azimuth.
- While IceCube muon rate is sensitive to variation in  $T_{\text{eff}}$ , it is generally insensitive to surface pressure changes.

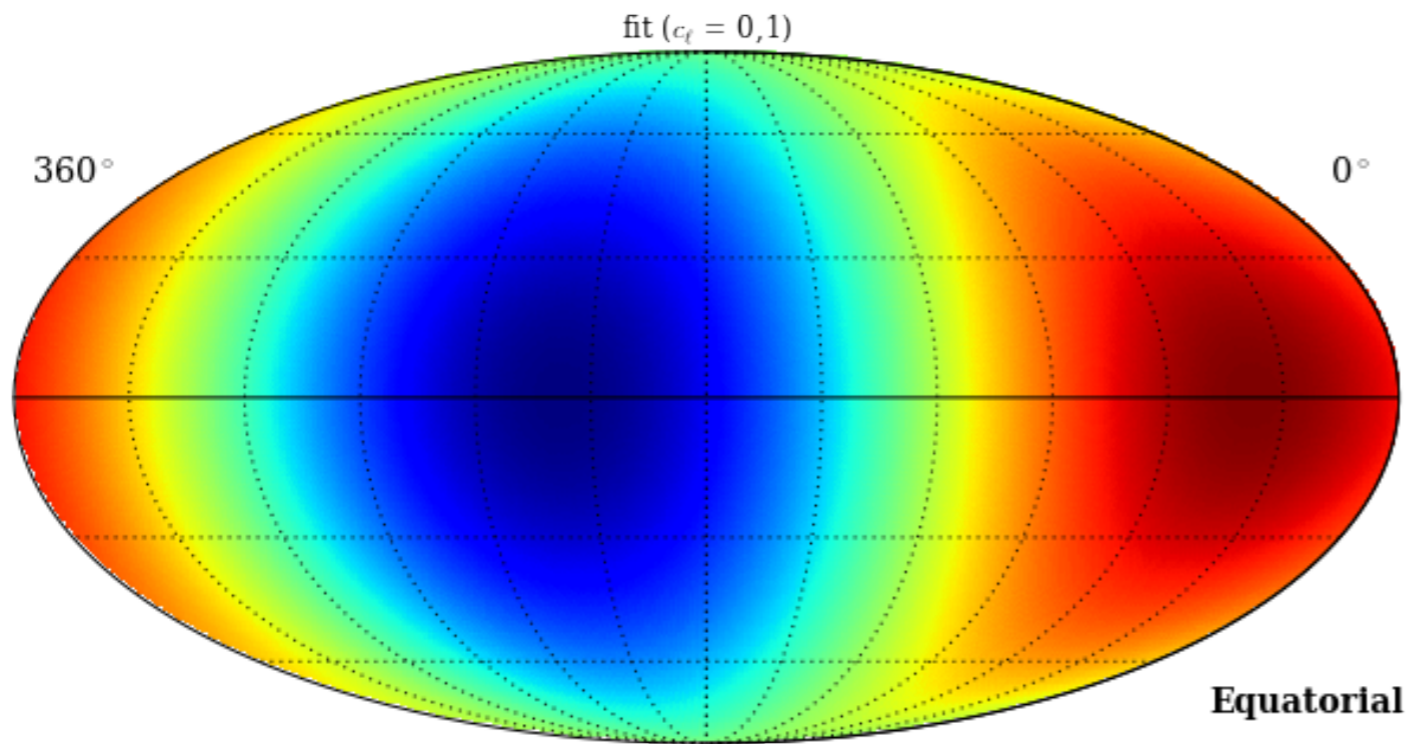


# Overlapping Region

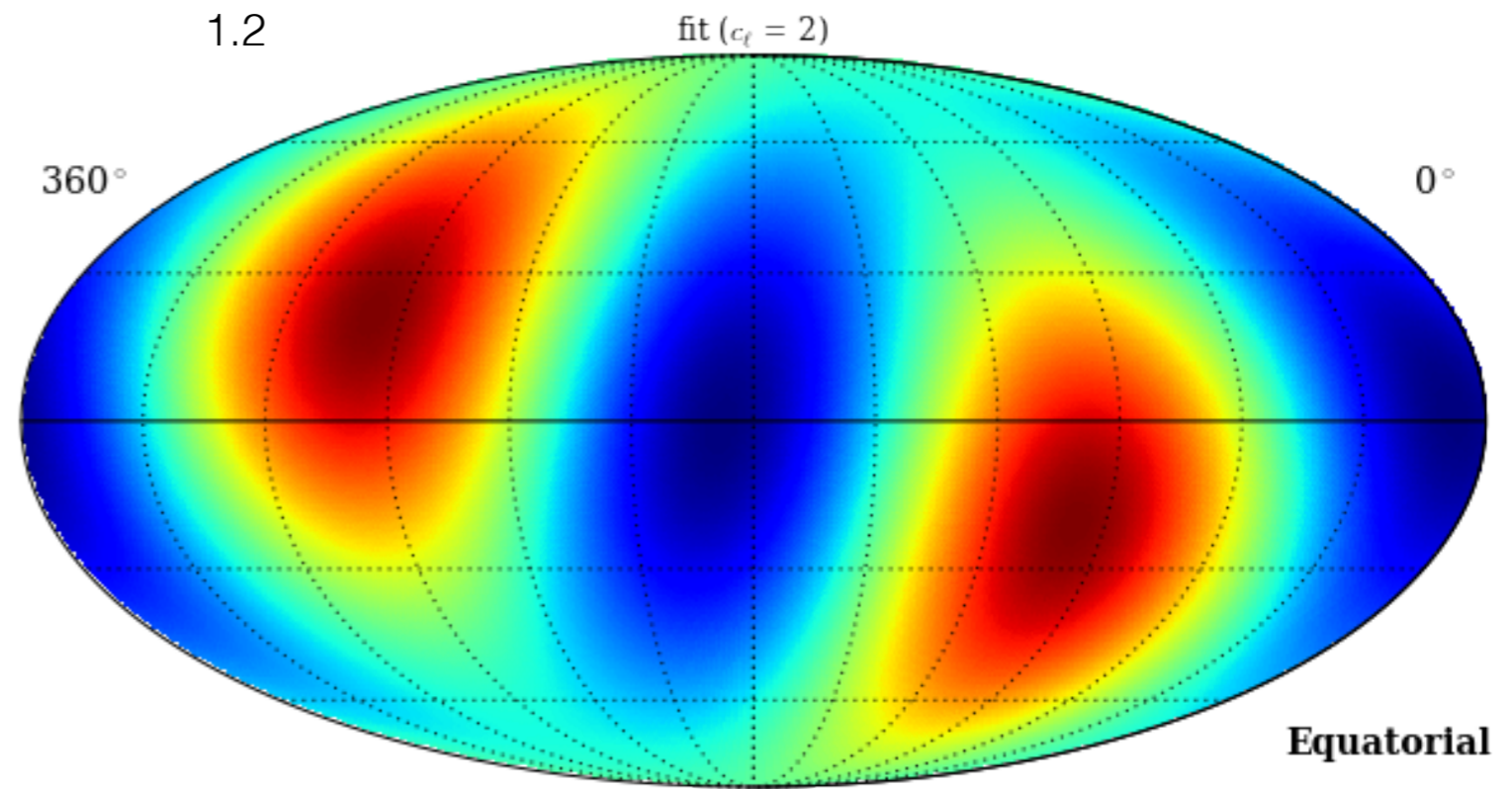
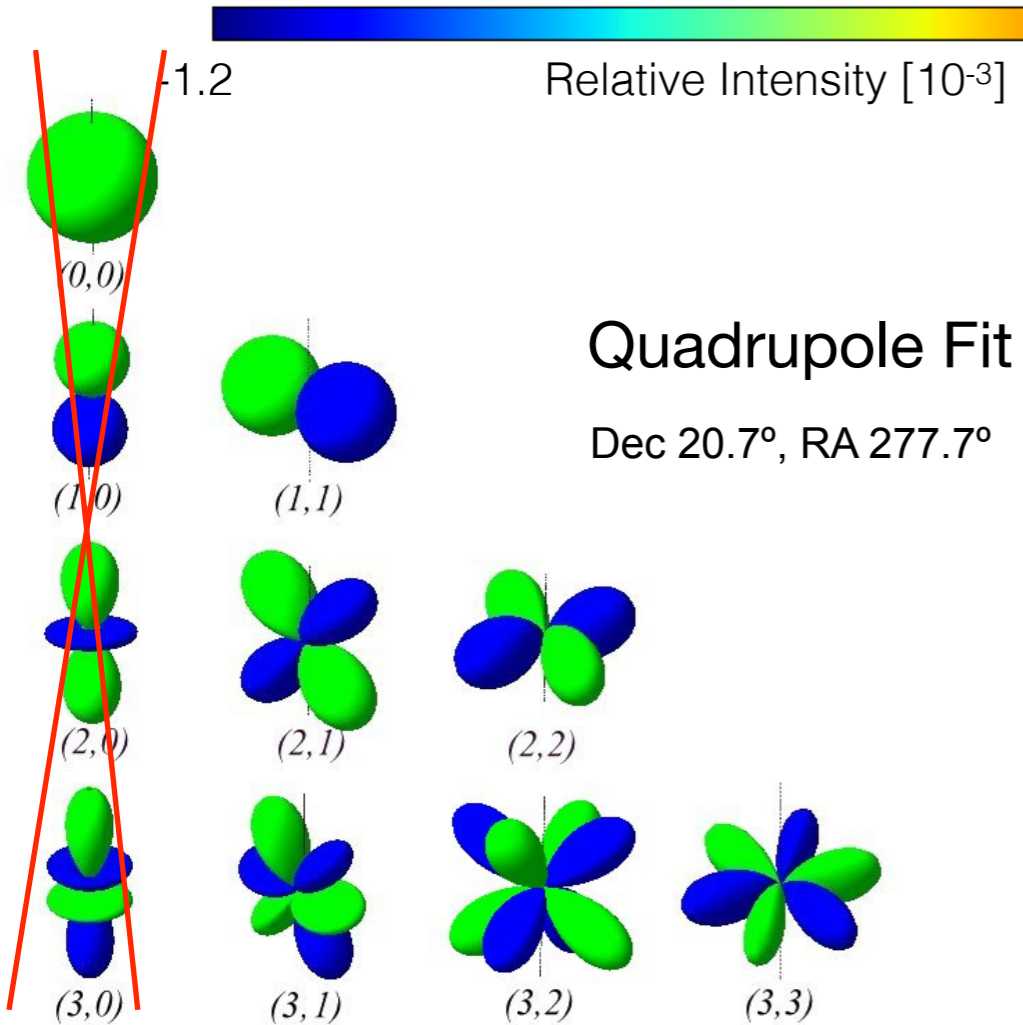


- Adjacent, overlapping  $\delta$  bins at  $-20^{\circ}$  for HAWC-300 and IC86 data.
- There is general agreement for large scale structures.
- The two curves correspond to different  $\delta$  bands but some differences in the small scale structure might also be attributed to mis-reconstructed events that migrate from nearby  $\delta$  bins with larger statistics as well as possible energy and composition differences.





Dipole Fit



-5.8  
33

Relative Intensity [ $10^{-4}$ ]

5.8

# IC86 2011-2016

- Data duration.
  - 5 continuous years
  - 2011-05-13 to 2016-05-20.
- Reconstructed a South Pole with fast but not very precise algorithms before being transmitted.
- Select long tracks with better angular reconstruction.
- Reconstructed energy  $< 32$  TeV.

## Data Cuts

- $\log_{10}(E_{\text{reco}}) < 4.5$  (32 TeV)
- $r\log l^* < 15$
- $l_{\text{dir\_c}}^{**} > 200 \cos(\theta_{\text{zenith}})$
- $n_{\text{dir\_c}}^{***} > 9 \cos(\theta_{\text{zenith}})$

\*Reduced log-likelihood of the track reconstruction fit.

\*\*Length of track in direct (on-time) PE hits.

\*\*\*Number of direct (on-time) PE hits.

# HAWC300 2015-2017

- Data duration.
  - 519.0 cont. day periods (653 total days)
  - 2015-05-01 to 2017-05-01
- Select high quality reconstructions.
- Eliminate  $\gamma$ -ray candidate events
- Reconstructed energy  $> 7.24$  TeV.

## Data Cuts

- $\log_{10}(E_{\text{reco}}) \geq 3.86$  (7.24 TeV)
- $n_{\text{Hit}}^* \geq 75$
- $0 \leq \theta_{\text{zenith}} < 1.0$  ( $57.3^\circ$ )
- $C_{\text{xPE40XnCh}}^{**} > 40$
- $\text{PINC}^{***} > 1.8$

\*Number of PE hits.

\*\*Number of channels beyond 40m from the reconstructed core.

\*\*\*Gamma/Hadron separation (smoothness of shower).

# Generalization for multiple observatories

In the case where you have multiple observations with common pixels, the optimal fit of the relative acceptance  $\mathcal{A}(0)$  and the background rate  $\mathcal{N}(0)$  of the null hypothesis becomes

$$\mathcal{N}_{\tau}^{s(0)} = \sum_i w_i^s n_{\tau i}, \quad \mathcal{A}_i^{s(0)} = \sum_{\tau} w_i^s n_{\tau i} / \sum_{\kappa j} w_j^s n_{\kappa j}.$$

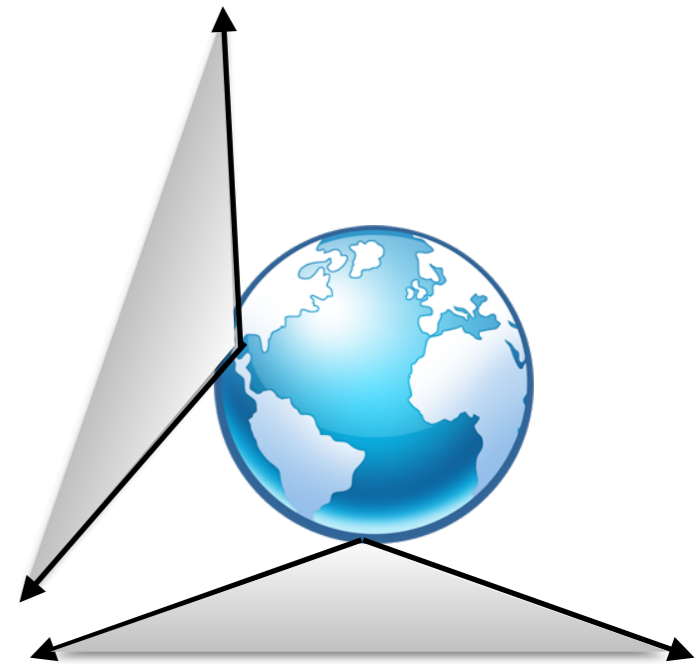
Where  $\mathbf{s}$  corresponds to the index of the observatory.

Then the maximum of the signal hypothesis obeys the implicit relation

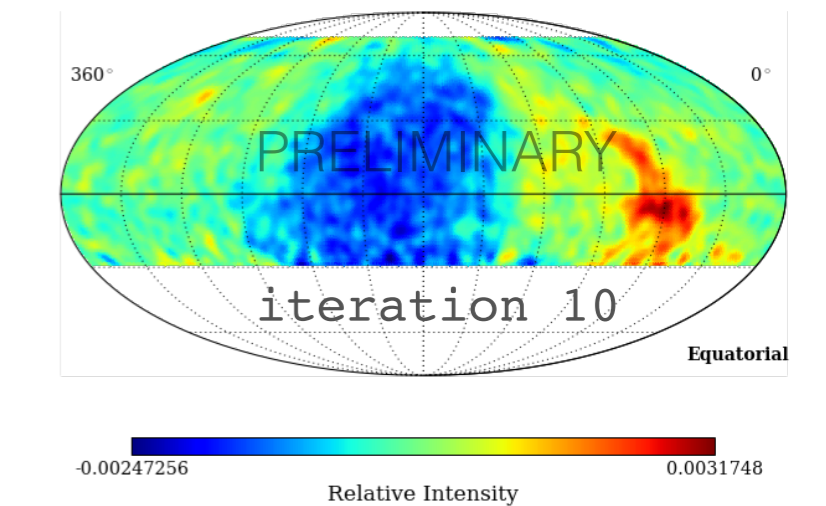
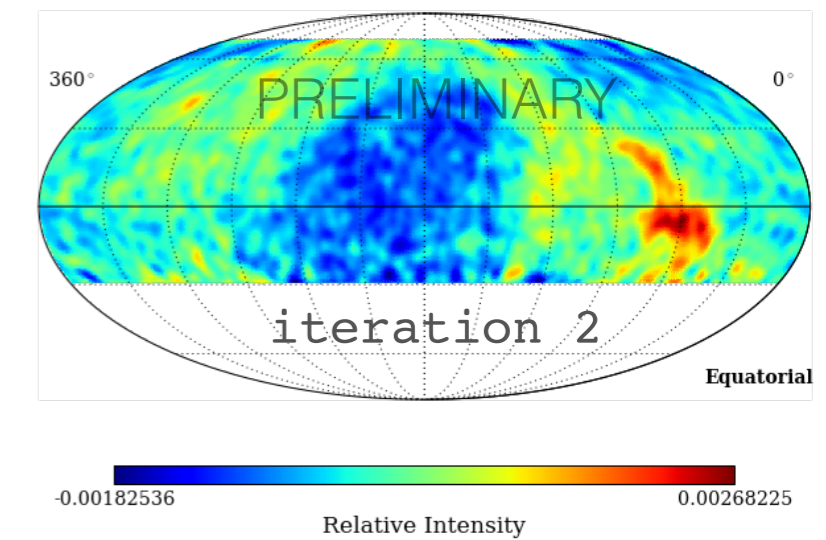
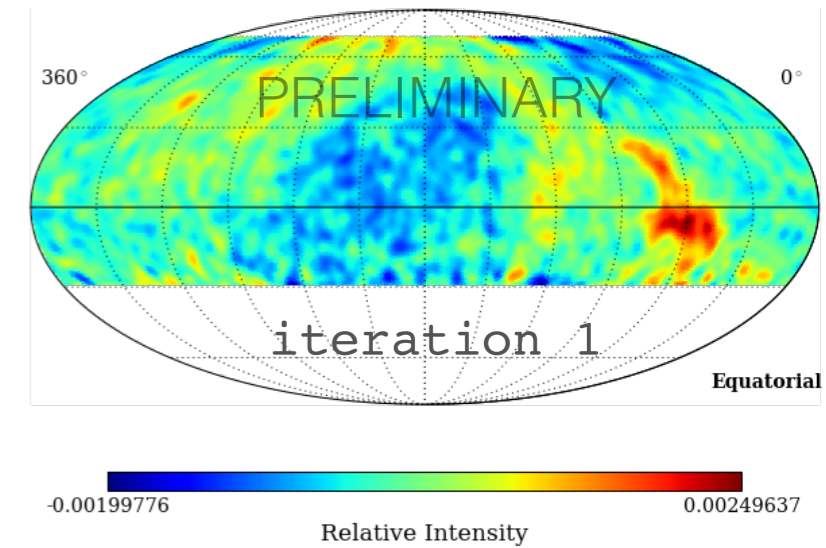
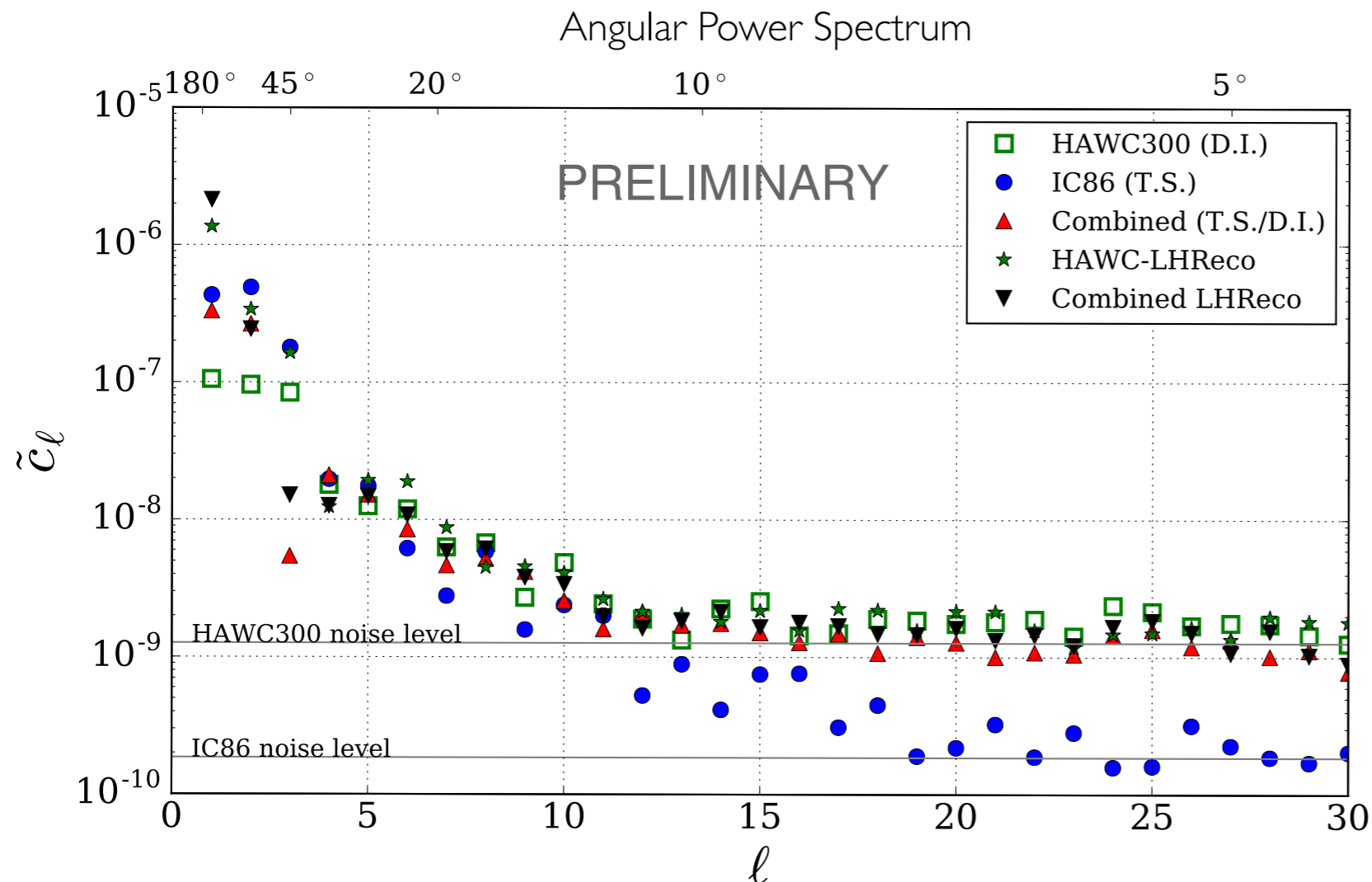
$$I_{\mathbf{a}}^* = \sum_{\tau} n_{\tau \mathbf{a}} / \sum_{s\kappa} \mathcal{A}_{\kappa \mathbf{a}}^{s*} \mathcal{N}_{\kappa}^{s*},$$

$$\mathcal{N}_{\tau}^{s*} = \sum_i w_i^s n_{\tau i} / \sum_j \mathcal{A}_j^{s*} I_{\tau j}^*,$$

$$\mathcal{A}_i^{s*} = \sum_{\tau} w_i^s n_{\tau i} / \sum_{\kappa} \mathcal{N}_{\kappa}^{s*} I_{\kappa i}^*.$$



- Iterative method recovers most of the power of large scale structure in mid-latitude observatories like HAWC.
- No appreciable gain for IceCube.
- The highest angular power for  $\ell = 1$  is obtained with the greater sky coverage from combining data from both observatories and reconstruction with the iterative method.

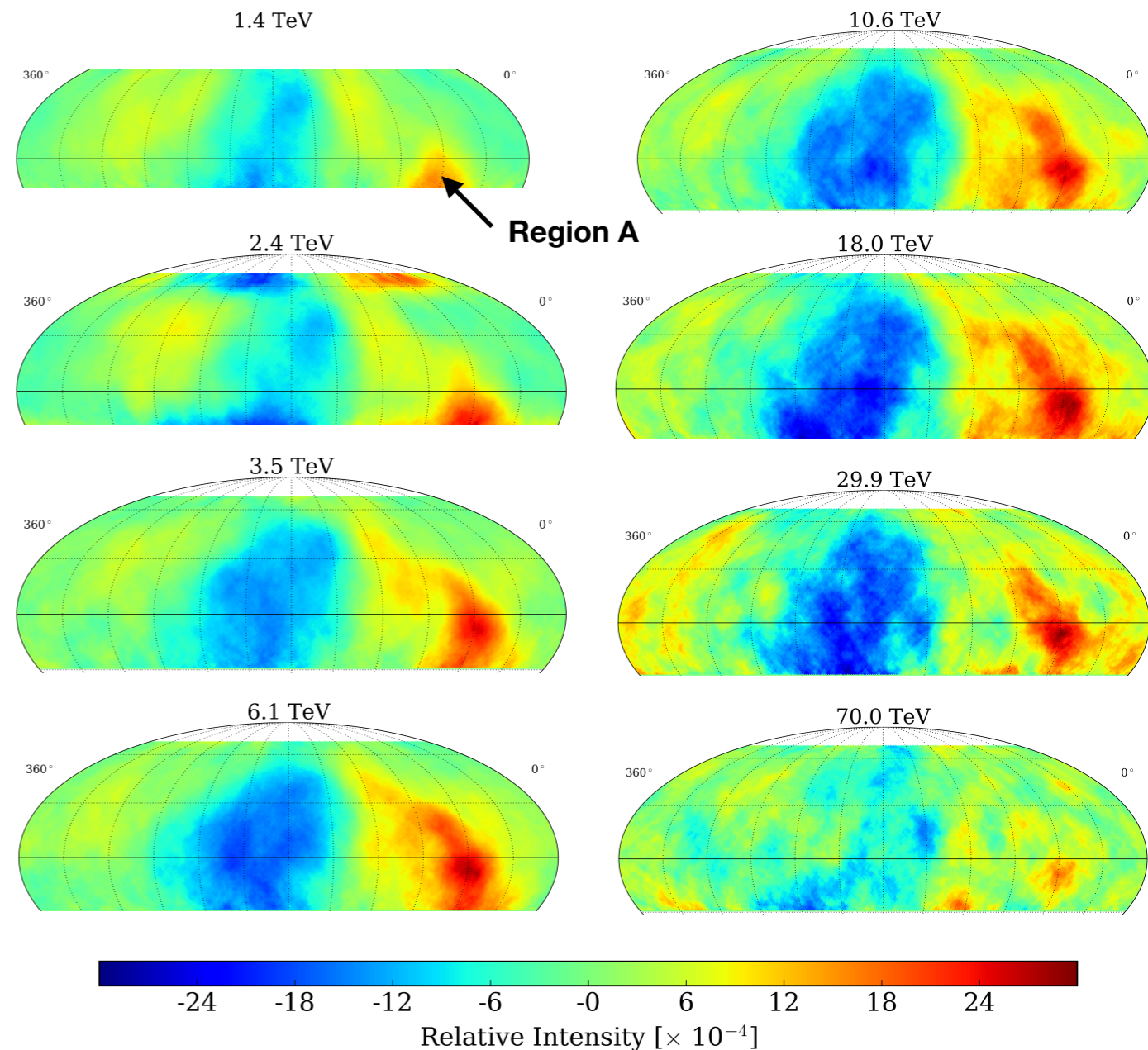


# HAWC Results



## Relative Intensity

- 400 full, sidereal days of HAWC data.
- Applied strong cut (2% pass) to reach unprecedented energy resolution for this measurement.
- LLH method to reconstruct CRA.
- Described using full 2D dipole fit (truncated).



Energy [TeV]	Amplitude [ $10^{-4}$ ]	Phase [ $^{\circ}$ ]	$a_{1,1}$ [ $10^{-4}$ ]	$a_{1,-1}$ [ $10^{-4}$ ]
2.5 $\begin{pmatrix} -1.2 \\ +3.5 \end{pmatrix}$	$3.21 \pm 0.16$	$7.9 \pm 2.9$	$-9.20 \pm 0.47$	$-1.28 \pm 0.47$
3.9 $\begin{pmatrix} -1.8 \\ +4.8 \end{pmatrix}$	$3.64 \pm 0.19$	$30.1 \pm 3.0$	$-9.12 \pm 0.55$	$-5.30 \pm 0.55$
6.3 $\begin{pmatrix} -2.7 \\ +6.4 \end{pmatrix}$	$8.84 \pm 0.21$	$37.5 \pm 1.3$	$-20.30 \pm 0.60$	$-15.57 \pm 0.60$
10.1 $\begin{pmatrix} -4.0 \\ +8.7 \end{pmatrix}$	$12.05 \pm 0.25$	$40.7 \pm 1.2$	$-26.44 \pm 0.72$	$-22.73 \pm 0.72$
16.3 $\begin{pmatrix} -6.1 \\ +12.1 \end{pmatrix}$	$12.19 \pm 0.32$	$41.0 \pm 1.5$	$-26.61 \pm 0.94$	$-23.15 \pm 0.94$
26.1 $\begin{pmatrix} -9.1 \\ +17.1 \end{pmatrix}$	$14.54 \pm 0.44$	$41.2 \pm 1.7$	$-31.69 \pm 1.26$	$-27.70 \pm 1.26$
40.3 $\begin{pmatrix} -13.3 \\ +24.3 \end{pmatrix}$	$13.78 \pm 0.60$	$27.9 \pm 2.5$	$-35.25 \pm 1.72$	$-18.65 \pm 1.73$
128.6 $\begin{pmatrix} -54.9 \\ +129.0 \end{pmatrix}$	$4.92 \pm 0.60$	$35.3 \pm 7.0$	$-11.62 \pm 1.74$	$-8.23 \pm 1.74$

# HAWC Results



## Statistical Significance

- Northward strengthening of 'Region A'
- Non-dipolar structure is obviously present
- Strong quadrupole component at low energies Run out of statistics in last bin...
- Compares favorable with other experiments when considering uncertainty in energy.

